THE PHOTODISSOCIATION PROCESSES OF KETENE

AT 3130 $\overset{o}{A}$, 3340 $\overset{o}{A}$ AND 3650 $\overset{o}{A}$

by

GLADSTONE ALTAMONT TAYLOR

B.Sc., McMaster University, 1958

A THESIS SUBMITTED IN PARTIAL FULFILMENT OF

THE REQUIREMENTS FOR THE DEGREE OF

MASTER OF SCIENCE

in the Department

of

Chemistry

We accept this thesis as conforming to the

required standard

THE UNIVERSITY OF BRITISH COLUMBIA

April, 1961

In presenting this thesis in partial fulfilment of
the requirements for an advanced degree at the University of
British Columbia, I agree that the Library shall make it freely
available for reference and study. I further agree that permission
for extensive copying of this thesis for scholarly purposes may be
granted by the Head of my Department or by his representatives.
It is understood that copying or publication of this thesis for
financial gain shall not be allowed without my written permission.

Department of _____CHEMISTRY_____

The University of British Columbia,
Vancouver 8, Canada.

Date___8th May 1961_____

ABSTRACT

Previous research on the photolysis of ketene has shown that the kinetics of photodissociation processes were not fully understood and that more accurate data were needed to evaluate the mechanism of the rate of dissociation of the electronically and vibrationally excited molecules.

There was some evidence that the primary quantum yields at shorter wavelengths extrapolated to a value greater than unity at zero pressure. if this were not within experimental error, it would provide evidence for a process of multistage deactivation of the excited ketene molecules.

In the kinetic studies of the dissociation of excited molecules, intersystem crossing to the triplet state had been included to account for phosphorescence. Theoretical consideration from this had led to predictions of the effect of dissociation from the triplet state on the quantum yields of carbon monoxide on the photodissociation of ketene. Experimental verification was now needed to determine the effect, if any, derived from triplet dissociation.

Previous attempts have been made to apply the unimolecular theory of dissociation to the photodissociation of excited molecules, but the data available yielded physically impossible results. Hence, only reasonable theoretical values of the parameters involved are given.

This research attempted to obtain more accurate data on the quantum yields of ketene at 3130 $\overset{o}{A}$, 3340 $\overset{o}{A}$ and 3650 $\overset{o}{A}$ at various temperatures.

From the results it is now possible to differentiate within the limits of the experiment, between the various theories of the dissociation process. It is established that triplet dissociation is either not a real effect or is small enough to be undetectable under the experimental conditions.

It is possible to discount a theory of a cascade collisional deactivation process involving more than three collisions of the excited molecules, but differentiation is not made between one, two and three collisions under experimental conditions.

The unimolecular theory of dissociation is applied to the results of the photodissociation process and values determined for the parameters involved. Reasonable agreement with the theoretical predictions is obtained.

TABLE OF CONTENTS

LIST OF FIGURES

LIST OF TABLES

ACKNOWLEDGMENT

The author wishes to express sincere thanks to Dr. G. B. Porter under whose supervision this investigation was carried out and whose unselfish help and guidance made this investigation fruitful.
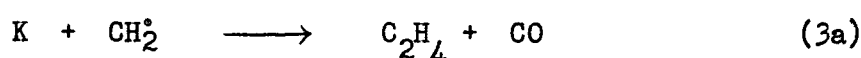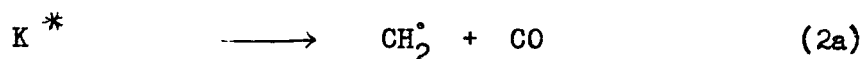
My sincerest thanks go to my wife for her co-operation and encouragement throughout this research.

My appreciation also goes to Mrs. E. Hinke who was remarkably patient in typing and proof-reading this thesis.

INTRODUCTION

1. **Early Work**

The earliest photochemical decomposition of ketene was done by Norrish, Crone and Saltmarsh[1]. These workers showed that carbon monoxide and ethylene were produced in a ratio of 2:1 and postulated the reaction as

$$K + h\nu \longrightarrow K^* \qquad (1a)$$

$$K^* \longrightarrow CH_2^{\cdot} + CO \qquad (2a)$$

$$K + CH_2^{\cdot} \longrightarrow C_2H_4 + CO \qquad (3a)$$

where K is the ketene molecule and K^* the excited state. Ethylene was formed by reaction between methylene radical and ketene rather than by association of methylene radicals.

This mechanism was disputed by Ross and Kistiakowsky[2] who suggested because of the large amount of activation energy probably required, reaction 3a did not occur to any extent and that the ethylene formed was then due to the combination of methylene radicals. On this basis, the quantum yield would then be unity instead of 2 as from Norrish and co-workers.

Further work by Pearson, Purcell and Saigh[3] seemed to confirm this view as they found that a) each methylene radical survived 4×10^5 collisions with ketene molecules in the quartz reaction vessel, and b) the mean value of 1.08 as found by Kistiakowsky and Ross could not be safely assumed to exceed unity in view of the experimental errors involved. Hence it was likely that, the reaction between methylene and ketene being slow, methylene was removed by association.
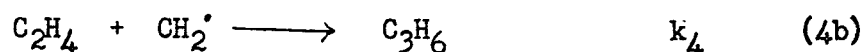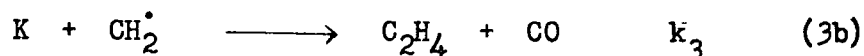
It had also been observed that if the photolysis and consequent dissociation was done in the presence of ethylene, a non-volatile polymer was formed, presumably by attack of $CH_2^{\bullet}$ radicals on the ethylene.

The work of Rosenblum[4] further supported methylene association. Methylene radicals had been known to react with other methylene radicals[1,5] to form ethylene, and with ethylene itself[1,6] to yield polymeric unsaturated hydrocarbons. The absence of methylene during thermal decomposition of methane was attributed to radical combination. Also methylene radical combination with carbon monoxide had long been known[6].

Rosenblum showed that photolysis of ketene in the presence of methane, ethane and ethylene, increased polymer formation. Photolysis in the presence of hydrogen also yielded a condensed polymer and higher saturated hydrocarbons, and no reaction occurred when hydrogen and ethylene were irradiated together. This indicated that methylene radicals could polymerize hydrocarbons.

2. Later Work

Subsequent evidence[7-10], however, confirmed the scheme first proposed by Norrish, Crone and Saltmarsh[1]. In one work by Kistiakowsky and Rosenberg[7], the reaction was studied by irradiating mixtures of ethylene and ketene. With methylene-ethylene reaction there would be no pressure rise, with the result that as the ethylene/ketene ratio in the reaction cell is increased, the rate of pressure rise is lowered. By using a large excess of ethylene, it was insured that the methylene formed by decomposition of ketene would react almost exclusively with the ethylene. Under these conditions the pressure of the system remained constant indicating little if any polymerization of ethylene. The reactions could then be written

$$K + h\nu \longrightarrow CH_2^\bullet + CO \qquad I_a \qquad (1b)$$

$$2CH_2^\bullet \longrightarrow C_2H_4 \qquad k_2 \qquad (2b)$$

$$K + CH_2^\bullet \longrightarrow C_2H_4 + CO \qquad k_3 \qquad (3b)$$

$$C_2H_4 + CH_2^\bullet \longrightarrow C_3H_6 \qquad k_4 \qquad (4b)$$
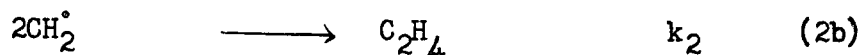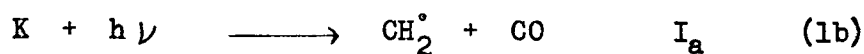
From steady state assumptions, if reaction 3 was neglected, we have

$$R = 1 - Z \left(1 + \frac{2}{Z}\right)^{1/2} \qquad \text{where} \quad Z = \frac{k_4^2 (C_2H_4)^2}{4k_2 I_a} \qquad (1)$$

and R is the ratio of the rate of pressure change on irradiation of a given mixture of ethylene and ketene to the rate of pressure change in pure ketene at the same pressure as the ketene in the mixture.

If reaction 2b was neglected rather than reaction 3b we have

$$R = \frac{1}{1 + \frac{k_4 (C_2H_4)}{k_3 (K)}} \qquad (2)$$

Thus the effect of light intensity offered a basis for neglecting one of the two reactions. A plot of R as a function of ethylene/ketene ratio at two different intensities showed no effect of different intensities.

An important difference in reactions 2b and 3b also is embodied in the rate of carbon monoxide production. If reaction 2b predominates, the rate should be independent of the ethylene/ketene ratio. If reaction 3b predominates the rate should decrease at higher ethylene/ketene ratios, approaching a limit of one half of that obtained for pure ketene. Investigation showed that the rate of carbon monoxide production does fall off with increasing ethylene/ketene mixture, although not to the extent predicted from reactions 1b, 2b, and 4b.

This evidence definitely established that reaction 2b did not occur and it was concluded that methylene radicals did not undergo an association reaction but reacted with ketene or with ethylene under the conditions of the experiment. In pure ketene the ratio of moles of carbon monoxide formed to the moles of ethylene formed from reaction 3b was 2.19 ± 0.02.

The temperature independence of ratio R indicated that the activation energies of the reactions of methylene with ketene and with ethylene were nearly identical. The ratio of these rate constants (k_4/k_3) had the value 2.5. The same ratio was obtained for the reaction of propylene with methylene. Thus not only the activation energy of the three reactions but also their frequency factors were the same. This was improbable if the products were as simple as reactions 3b and 4b suggested. This led Kistiakowsky and Rosenberg[7] to propose diradical formation in the first elementary steps of all three cases: $CH_2CH_2CO\cdot$, $CH_2CH_2CH_2^\cdot$ and $CH_2\overset{\cdot}{C}HCH_3$, a conclusion which was further supported by a) the imperfect agreement between predicted and observed effect of ethylene/ketene ratio on the rate of carbon monoxide formation, and b) inconstancy of the ratio of rate constants k_4/k_3 which varied from $2\cdot3$ to $3\cdot1$.

Later work by Kistiakowsky and co-workers[10] showed that methylene radicals reacted with ethylene and with carbon monoxide to form propylene and ketene respectively. The formation of ketene from methylene radicals and carbon monoxide explained the pronounced drop of rate of pressure rise on protracted irradiation of ketene.

Kistiakowsky and co-workers[7,10] had also shown that quantum yields in ketene decomposition increased with decreasing wave length. At 2700 Å Strachan and Noyes[11] found that within experimental error the primary

quantum yield was unity and there was no significant variation with temperature or pressure. At 3650 Å there was a marked dependence of the primary quantum yield on pressure and temperature, decreasing with increasing pressure and increasing with increase in temperature, and was much less than unity when extrapolated to zero pressure of ketene. At 2700 Å the quantum yield of carbon monoxide formation was 2.12 ± 0.15. This was to be expected if reactions 1a, 2a and 3a were the sole ones.

In agreement with the value of 2.19 obtained by Kistiakowsky and co-workers[7], they found that the average ratio of carbon monoxide to ethylene in the products was 2.20. This difference from the expected value of 2 from reactions 1a, 2a and 3a was due to additional reactions whose rates were essentially independent both of ketene pressure and temperature. These reactions could be of the form

$$K + CH_2^{\cdot} \longrightarrow CH_2)_2CO^{\cdot} \qquad (1c)$$

$$M + CH_2)_2CO^{\cdot} \longrightarrow polymer + CO + M \qquad (2c)$$
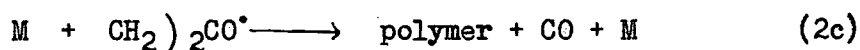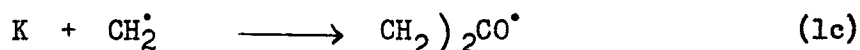
where M could be either ketene or ethylene.

At 3650 Å the low quantum yields observed were attributed to (a) internal conversion and (b) collissional deactivation between ketene molecules occurring along with the primary dissociation process:

$$K + h\nu \longrightarrow K^* \text{ (excitation)} \qquad (1d)$$

$$K^* + K \longrightarrow 2K \text{ (collisional deactivation)} \qquad (2d)$$

$$K^* \longrightarrow products \text{ (dissociation)} \qquad (3d)$$

$$K^* \longrightarrow K \text{ (+ } h\nu \text{ ?) (internal conversion)} \qquad (4d)$$
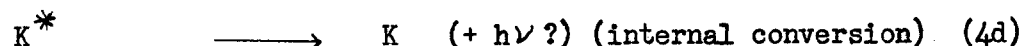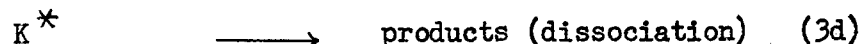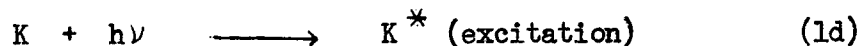
where K is a ketene molecule and K^* the excited state.

3. Recent Work

A more extensive study of photochemical processes was done by Noyes, Porter and Jolly[12] and by Porter[13] who investigated the internal

conversion process and the possibility that a radiationless transition
occurred from the excited electronic state to an upper vibrational level
of the ground electronic state, followed by rapid collisional deactivation
because no fluorescence as suggested by reaction 4d had been observed.

The mechanism for a photochemical reaction that proceeded via
excited molecules could be represented by the following reactions, consid-
ering only one excited electronic state.

$$X + h\nu \longrightarrow Y_n \qquad (1e)$$

$$Y_n + M \longrightarrow X + M \qquad (2e)$$

$$Y_n \longrightarrow D \qquad (3e)$$

$$Y_n \longrightarrow X_m \qquad (4e)$$

$$X_m \longrightarrow Y_n \qquad (5e)$$

$$X_m \longrightarrow X_i \qquad (6e)$$

$$X_i \longrightarrow X_m \qquad (7e)$$

$$X_i + M \longrightarrow X + M \qquad (8e)$$

X is a molecule, e.g. ketene in its ground state in thermal equilibrium
with surrounding molecules; Y_n is a molecule in upper vibronic state reached
by absorption of radiation; D represents the dissociation products (in this
case carbon monoxide and methylene radicals). M is a molecule capable of
degrading vibrational energy by collision; X_i represents those molecules in
higher vibrational levels of the ground state having the same total energy
as Y_n. There would be many degenerate states corresponding to X_i, but only
a few designated by X_m will have a configuration such that a radiationless
transition to Y_n has a high probability. A molecule X_i will spend only a
small fraction of its lifetime in configuration X_m. X_m is the state formed
when a molecule Y_n makes a transition to the ground electronic state
(reaction 4e). Internal conversion was considered to have occurred when

reaction 8e had removed sufficient energy from X_m to prevent its return to Y_n.

Primary quantum yields calculated from the above was the same as the simpler mechanism suggested by reactions 1d, 2d, 3d and 4d as long as the concentration was high enough such that $k_8(M) \gg k_7$. Since the relationship was not valid in the low concentration region, the quantum yield should increase with decreasing concentration, and should be unity on extrapolation to zero pressure. k_7 was also assumed to be small compared to $k_8(M)$ since the quantum yield was found independent of concentration. Thus all excited ketene molecules that made the transition from Y_n to X_m were subsequently deactivated by collision even at the lowest concentration studied.

Since no fluorescence had ever been observed, it must be assumed that the energy in the internal conversion and collisional deactivation processes was lost as heat. Extrapolation to zero pressure gave a carbon monoxide quantum yield of about 0.06. The low quantum yield values obtained suggest that internal conversion is more rapid than dissociation. With increase of pressure collisional deactivation becomes the more dominant process. At 3650 $\overset{o}{A}$ it appears that dissociation occurs only after a finite time interval long enough for the ketene molecule to be deactivated.

The variation of quantum yield with pressure at 3130 $\overset{o}{A}$ and 3340 $\overset{o}{A}$ was investigated by Connelly and Porter[14,19]. At 3130 $\overset{o}{A}$ it was found that the conclusion of Kistiakowsky and Mahan[15] that the quantum yield was independent of pressure and possibly equal to unity applied only to low pressure measurements. A plot of the reciprocal of the primary quantum yield against pressure revealed a positive slope. The primary quantum yield was 1.0 at pressures up to 60 mm but decreased to 0.59 at 750.7 mm

pressure. At low pressures, the ketene molecule dissociated to form products, but at higher pressures collisional deactivation became a noticeable factor. The ratio of quantum yield of carbon monoxide to ethylene was found to be approximately 2.14 at 2700 Å, 3130 Å and 3650 Å.

At 3340 Å the quantum yield was found to be 0.72 at 26 mm and 0.21 at 384 mm. A similar plot to 3130 Å yielded a much steeper slope indicating considerable collisional deactivation. A larger intercept was also obtained, which was interpreted from the mechanism as evidence that internal conversion was also a contributing factor. The slope and intercept decreased with increase of temperature and the activation energy of dissociation was found to be about 2 k cals/mole. At 3650 Å, the intercept and slope also decreased with increase of temperature and the activation energy was about 4.5 k cals/mole.

4. Object of Present Investigation

As more accurate data were needed to evaluate the photochemical processes involved, it was decided to investigate the photolysis of ketene using experimental technique which would give more accurate measurements of quantum yields than had previously been obtained.

It was hoped that this data would lead to a better understanding of the collisional deactivation process. In the dissociation process discussed by Porter and Connelly[19] it was shown that if the collisional deactivation process involved a "strong collision" i.e., each excited molecule was deactivated by a single collision with an unexcited molecule the plot of the inverse quantum yield against pressure would be a straight line and the data assumed to fit the equation

$$1/\phi = 1 + (k_{2n}/k_{1n})K$$

or at longer wave lengths, the equation

$$1/\phi = 1 + (k_{3n}/k_{1n}) + \frac{k_{2n}(K)}{k_{1n}}$$

where k_{1n} = rate constant for dissociation

k_{2n} = rate constant for collisional deactivation

k_{3n} = rate constant for internal conversion

ϕ = quantum yield of carbon monoxide

However, if the collisional deactivation process was a "weak collision" process i.e., a cascade collisional process in which each excited molecule lost its energy by a series of collisions, a plot of $1/\phi$ against pressure from the equations derived for the process, would, at low excitation energies yield linear curves. At higher excitation energies, the curves would be linear only in the high pressure regions and would be concave upwards at low pressures. As the number of degradational collisions increased, aside from the increased quantum yields, departure from linearity would increase and a higher extrapolated quantum yield to zero pressure obtained.

If the process also involved a single collisional degradation, the simple Kassel theory of unimolecular dissociation could be applied to the photodissociation. Hence from the results it would be possible to evaluate in reasonable terms the parameters ν, ε_m and ε_{o-o} involved. However, if the process was a cascade one, application of the simple unimolecular theory would be impossible as more parameters would be needed.

Finally it was felt that an investigation of the effect of temperature variation would also be valuable. The variation observed, if any, would give information as to the extent of triplet dissociation, this interstate crossing from singlet to triplet, having been introduced in the

kinetic study of excited molecules to account for the observation of phosphorescence.

From the theory, at low pressures a plot of the inverse quantum yield against pressure should be linear and correspond to singlet dissociation because collisional excitation and consequent dissociation in the triplet state would be negligible.

With increase of temperature and consequent increase in the number and energies of molecular collisions, collisional excitation, and consequently dissociation from the triplet state should become increasingly important. The plot of $1/\phi$ against pressure then should begin to depart from linearity and become concave downward.

EXPERIMENTAL

1. Light Source

A B.T.H. medium pressure mercury arc lamp was used in all the runs. The divergent beam was passed through a combination of two quartz plano-convex lenses to produce a parallel beam. The beam was then passed through a circular aperture 2 cm in diameter, which could be closed by a shutter when desired, and into a filter cell. This cell, was kept filled with distilled water by means of two side arms. At one end was a quartz window, and at the other a 3 mm Corning 9863 filter glass to exclude visible radiation. The beam was then passed through a circular aperture similar to the first, into the cell housing.

2. Cell Housing

The housing consisted of a brass box (see Fig. I), mounted by two supports on an optical bench on which the lamp and lens system were also mounted. The cell housing was divided into four main compartments. The first contained the filter cell and interference filter mentioned previously. It had a removable light tight cover.

The next compartment was further sub-divided into two sections, the dividing wall having a circular aperture 2 cm in diameter. The larger section contained a quartz plate 3.8 cm in diameter at an angle of 45° to the path of the light.

Most of the incident beam was transmitted into the reaction vessel but part was reflected into the smaller compartment which contained a mount for the actinometer cell immediately behind the aperture in the dividing wall.

FIGURE 1. Diagram of Cell Housing
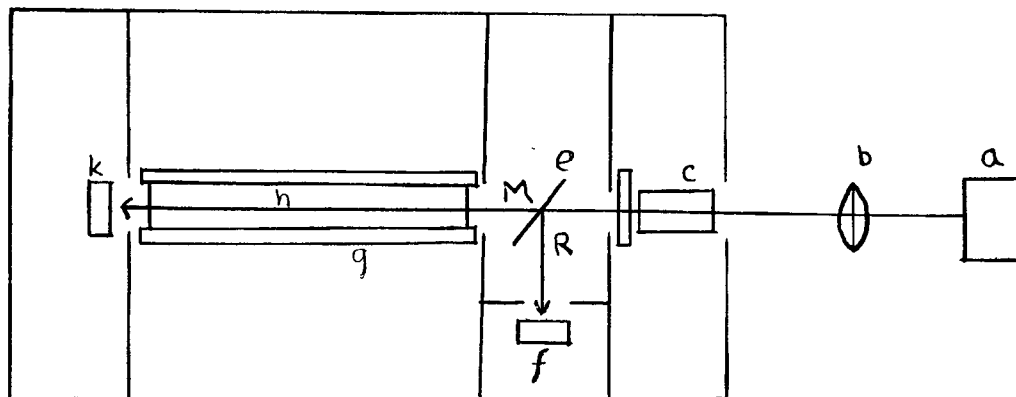
a. light source

b. plano-convex lenses

c. filter cell with water

d. Jena-Schott Interference filter

e. quartz window

f. actinometer cell (R)

g. temperature control housing for reaction vessel

h. quartz reaction vessel

k. actinometer cell (M)

R reflected beam

M transmitted beam

The transmitted beam then entered the next compartment through a circular aperture behind which the reaction vessel was placed. This compartment had a removable light-proof lid as previously described, to which the photolysis cell holder was fixed thus enabling the cell to be lifted out of the housing for cleaning and spectrometric measurements.

The brass cell holder consisted of an inner and an outer shell, the thickness being about 1 cm. The space between the shells consisted of a series of baffles (see Fig. 2). Water was passed through this system, thus giving temperature control of the reaction vessel, which was fitted exactly in the inner shell. The cell holder was made in two halves and soldered around the cell. To reduce heat transfer the cell holder was wrapped with glass wool.

The quartz reaction vessel, was placed as accurately parallel as possible in the path of the beam. Its sidearm was blackened to exclude external radiation and attached by means of a hollow bore high vacuum stop-cock to the vacuum system.

The fourth compartment contained a holder for the second actinometer cell, placed exactly behind a 2 cm hole, through which the beam after passage through the reaction vessel, entered the compartment.

3. <u>Drying System</u>

For runs at temperatures below room temperature condensation of moisture on the cell windows was prevented by ensuring that the air in this compartment was dry. A large aluminium tray was filled with Drierite and placed in this compartment. A constant circulation of dry air, entering through an inlet in the aluminium cover of the second compartment, and at the temperature of the reaction vessel, was kept up through this compartment.

FIGURE 2. Baffle System of Water Circulation in Cell Temperature Control Housing

out

coolant in
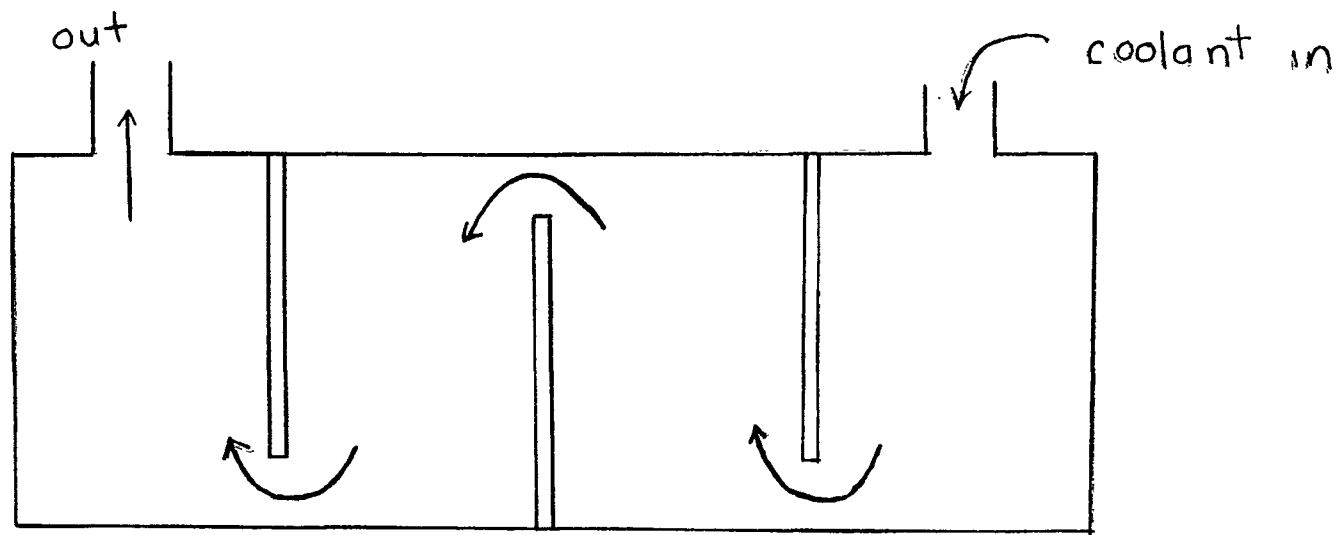
For this purpose, nitrogen from a cylinder was used in some of the shorter runs. For long runs pressurized air was passed through a series of large glass tubes with different drying agents--calcium chloride, Drierite and Anhydrone respectively. The air was then passed through another tube packed tightly with glass wool and then through a sintered glass disc to ensure that no dust particles entered the compartment. The air was cooled by allowing it to pass through a series of glass coils immersed in water at the same temperature as the reaction vessel.

4. Temperature Control System

This consisted of a 4.5 litre Dewar vessel containing water whose temperature was kept to within $\pm$ 1°C by adding either ice or tap water. A small circulating pump was fixed to a wooden base placed on the top of the Dewar, with the inlet well below the water level. The outlet was attached by a short piece of plastic tubing to the inlet pipe of the beffle circulatory system of the cell holder described previously. After circulation through the system, the water was returned through the outlet tube of the baffle system to the Dewar for cooling and recirculation. Runs at temperatures below 0°C were attempted, but were abandoned because of difficulties with the circulating system.

5. Filters

The various wavelengths used for photolysis were obtained by the use of Jena-Schott interference filters placed in a holder behind the filter cell. For runs at 3130 Å the interference filter had a λ_{max} = 310.5 μ, and $\overline{T}_{max}$ = 20%. For runs at 3340 Å, the filter had a λ_{max} = 331 μ and $\overline{T}_{max}$ = 36.5%. For 3650 Å wavelength λ_{max} = 365 μ and $\overline{T}_{max}$ = 38%. These were

prevented from getting too hot during long periods of exposure by the water in the filter cell mentioned earlier, which absorbed the infra-red ratiation.

6. Preparation and Purification of Ketene

Ketene was prepared on the vacuum system by pyrolizing acetic anhydride[16], as illustrated in Figure 3. By pumping on the acetic anhydride in the storage bulb, a slow stream of the vapor flowed through the oven, which was heated to $504^{\circ}C$. The acetic acid produced and the unused acetic anhydride were collected in a dry-ice-acetone bath on the low pressure side of the oven. The ketene was collected in a liquid nitrogen trap.

When enough ketene had been collected, it was purified by trap to trap distillation, the middle third being retained, then stored in a bulb immersed in liquid nitrogen to prevent polymerization. Before each run a quantity of ketene was transferred from the storage bulb, condensed by liquid nitrogen on a portion of the vacuum line, and outgassed three times, thus ensuring that all non-condensable or low boiling gases were removed.

7. Photolysis of Diethyl Ketone

Diethyl ketone was used as a primary standard to check the quantum yields obtained. A blackened bulb containing pure diethyl ketone was put on the vacuum line, outgassed as before, and by successive condensation on the side arm of the reaction vessel enough was transferred to the reaction vessel to give an absorption of about 40% of the incident light. Photolysis was done at 3130 Å and at $100^{\circ}C$, where the quantum yield of carbon monoxide is known to be 1.0[17].

This temperature was obtained by substituting the water in the circulating system by linseed oil, which was heated to the desired temperature by an electric coil inserted in the storage Dewar.

FIGURE 3. Preparation of Ketene by Pyrolysis of Acetic Anhydride at 504°C

a. acetic anhydride
b. pyrolysis vessel
c. aluminium furnace at 504°C
d. dry ice trap
e. liquid nitrogen trap for ketene
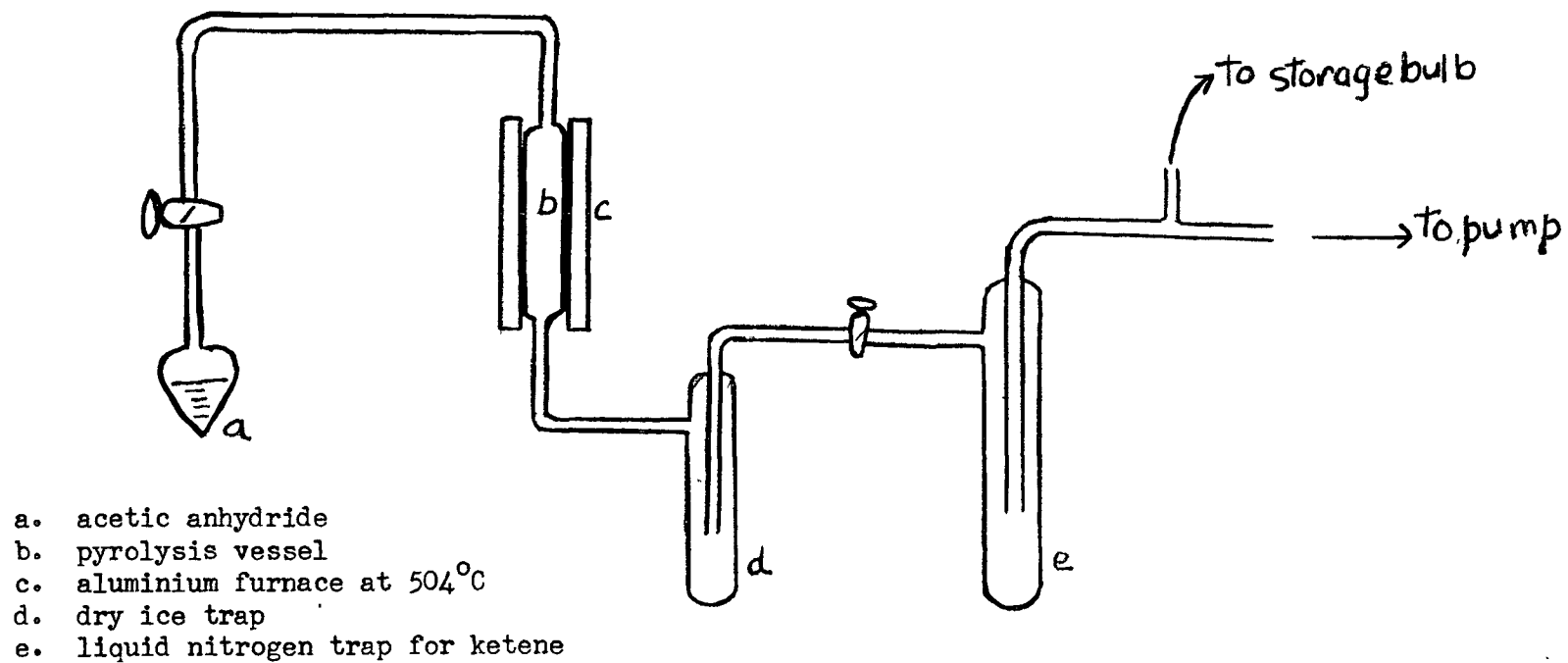
8. <u>Gas Analyses</u>

After photolysis, the gases were analysed in an all-glass vacuum system evacuated by a standard oil pump and a single stage mercury diffusion pump.

The analyses of carbon monoxide were performed by allowing the gases from the reaction vessel to flow through traps cooled to $-196^{\circ}C$ and $-211^{\circ}C$ (liquid nitrogen and solid nitrogen respectively). The solid nitrogen trap was obtained by pumping on fresh liquid nitrogen for about twenty minutes.

Ketene was condensed in the first trap and ethylene in the solid nitrogen trap. The carbon monoxide was not condensed at these temperatures and was measured by a McLeod-Toepler gauge similar to that used by Strachan and Noyes[11].

9. <u>Actinometry</u>

The intensity of the absorbed radiations at the various wavelengths was determined by the use of the potassium ferrioxalate actinometer as described by Hatchard and Parker[18]. The optical densities of the exposed solutions were carefully determined on a Unicam spectrometer at 5100 $\overset{o}{A}$ using 1 cm cells and were corrected for the 'blank' of the unexposed solution.

During exposure about 5 ml of the ferrioxalate solution were put in the actinometer cells, and with the beam cut off, the cells were placed in position and then exposed by use of the lever mentioned earlier. The actinometer cells were about 2.4 cm in diameter and 1.5 cm in path length. They were blackened on all sides except the quartz window facing the incident light. After exposure the solutions were removed from the cells, the cells washed out three times with water and the washings added to the solution.

Because of the intensity of the radiation at 3130 $\overset{o}{A}$, exposure times were short and the exposed actinometer solution in the main beam was diluted to five times the volume of the other to obtain an optical density within an accurately determinable region on the spectrometer. At pressures of ketene greater than 10 cm, where absorption of the incident radiation was great, no dilution was made.

For runs at 3340 $\overset{o}{A}$, longer periods of exposure were made and dilutions were made as before.

For runs at 3650 $\overset{o}{A}$, where exposure times were very long, it was necessary to do two or three different actinometer exposures during one run and dilutions were made to fall within an accurate region on the spectrometer.

Before each run was performed, the photolysis cell was thoroughly evacuated. The actinometer cells were then filled, placed in position, and after exposure, developed, and the optical densities determined. The results were expressed in a ratio of the form

$$R_o = \frac{O.D. \ (M) \times F}{O.D. \ (R)}$$

where O.D. (M) = optical density of solution in beam M (see Fig. 1)

O.D. (R) = optical density of solution in beam R

F = dilution factor.

The cells were refilled with ferrioxalate solution and placed in position. Ketene was then introduced in the reaction vessel at the desired pressure, which was determined on a manometer, and photolysed. The optical densities of the actinometer solutions were again determined and expressed as a ratio

$$R_p = \frac{O.D.\ (M)xF}{O.D.\ (R)}$$

The ratio of R_o/R_p was proportional to I_o/I_t where I_o was the intensity of the incident beam in the reaction vessel and I_t of the transmitted radiation. These ratios were plotted against the pressure in cm. and the data from the absorption coefficient curve obtained expressed in the form

$$Log_{10}\ I_o/I_t = ZP$$

where Z = slope

P = pressure (in cm. of Hg) of ketene in the reaction

vessel.

From this the amount of light transmitted could be determined.

The quantum yields of Hatchard and Parker[18] were used to determine the absorbed intensities. Because of the large amount of reflection from the glass-air interfaces of the reaction vessel and the actinometer cells, it was necessary to apply a correction factor to obtain the absolute intensity of the absorbed radiation. Using the refractive index of quartz, and considering only first order reflections, the correction factor had the form

$$I_a/E = 1.112\ x\ \frac{(1 - \gamma)}{\gamma}\ (1 + 0.1006\ )$$

where I_a = intensity absorbed by ketene in the reaction vessel

E = optical density of actinometer solution in beam M

γ = fraction of light transmitted.

Whenever the R_o ratio varied too widely from a certain mean, indicating a build up of polymer formation, the cell was removed, its transmission determined on the Carey Spectronmeter, cleaned with alcoholic

KOH, and its transmission redetermined. A correction factor was then applied to the results.

RESULTS

Values were obtained for the molar extinction coefficient of ketene at the various wavelengths. These are shown in Table 1. The value at 3650 $\overset{o}{A}$ is much smaller than at the other wavelengths, and the maximum shows a shift towards shorter wavelengths as the temperature is decreased.

For pressures below 10 cm the extinction coefficient curves were linear with pressure. Above 10 cm pressure however, especially for 3130 $\overset{o}{A}$ there was a marked departure from linearity. Consequently, the quantum yields in the region above 10 cm are the average of the experimental and the calculated results from the curves.

3130 $\overset{o}{A}$

From determinations at $0^{o}C$ and pressures about 2 cm, a carbon monoxide quantum yield 1.78 was obtained. At pressures in the region of 20 cm the quantum yield decreased to 0.758.

At $23^{o}C$ the quantum yields were correspondingly higher and decreased from 1.87 at about 2 cm pressure to a value of 1.17 at about 20 cm pressure of ketene. The results are given in Tables 2 and 3.

The time of each photolysis varied from 13 minutes at lower pressures to 18 minutes at higher pressures. With the cell empty the ratio of the beams stayed fairly constant for about four photolyses. With more than four runs, however, the ratio would decrease quite rapidly due to a build up of polymer formation. The cell would then be removed and cleaned with alcoholic potassium hydroxide.

During each photolysis only a small fraction of the ketene was allowed to decompose (about 5 - 7 per cent) to ensure that the reaction of methylene radicals with ethylene would be small. The quanta absorbed varied

from 0.650 μ-Einsteins at about 1 cm. pressure to 3.78 μ-Einsteins at 20 cm. pressure.

3340 Å

The carbon monoxide quantum yields were determined at $23^{\circ}C$ (Porter, G.B., personal communication), and at $0^{\circ}C$. The data are summarized in Tables 4 and 5. Exposure times were much longer than at 3130 Å, varying from two to three hours. The quantum yields of carbon monoxide are lower than at 3130 Å and likewise decrease with pressure, varying from 1.25 at low pressures to 0.48 at high pressures at $23^{\circ}C$. The quantum yields at $0^{\circ}C$ were lower than at $23^{\circ}C$.

3650 Å (Porter, G.B., personal communication)

Because of the very small amounts of decomposition products obtained at this wavelength by previous workers[11], it was decided to photolyze for periods of from four to six hours to give accurately measurable quantities within the limit of experimental determination. Because of the long exposure times, it was necessary to use three or four different actinometer solutions during each run. The quantum yields are given in Table 6. As can be seen, they are very much lower than at 3130 Å and 3340 Å decreasing from a value of 0.0334 at 2 cm. pressure to 0.00516 at 24 cm. pressure. The intensities absorbed were correspondingly 2.91 μ-Einsteins and 14.85 μ-Einsteins.

TABLE 1

MOLAR EXTINCTION COEFFICIENTS FOR VARIOUS WAVELENGTHS

a) Reaction Vessel Temperature: $23.0^{\circ}C$

Wavelength	Extinction Coefficient
3130 Å	81
3340 Å	111
3650 Å	31

b) Cell Temperature: $0^{\circ}C$

Wavelength	Extinction Coefficient
3130 Å	82
3340 Å	103

TABLE 2

PHOTOLYSIS OF KETENE AT 3130 Å

Reaction Vessel Temperature   23.0°C

Run	Pressure of Ketene in mm.	Intensity absorbed Einstein x 10^6	$\phi = 1/2 \, \phi_{CO}$
14	22.0	0.744	0.935 ± 0.005
15	53.8	1.803	0.836 ± 0.004
16	96.8	2.598	0.752 ± 0.004
17	152.3	2.786	0.631 ± 0.030
18	198.0	3.080	0.586 ± 0.003
19	10.2	0.554	0.956 ± 0.005
20	35.2	1.492	0.863 ± 0.024
21	130.2	2.322	0.687 ± 0.004
22	164.3	3.424	0.635 ± 0.003

TABLE 3

PHOTOLYSIS OF KETENE AT 3130 $\overset{o}{A}$

Reaction Vessel Temperature $0.0\,^{o}C$

Run	Pressure of Ketene in mm.	Intensity absorbed Einstein x 10^6	$\phi = 1/2\,\overline{\phi}_{CO}$
25	11.2	0.650	0.941 ± 0.054
26	20.3	0.968	0.863 ± 0.005
27	29.4	1.262	0.836 ± 0.016
28	42.2	1.678	0.771 ± 0.011
29	47.0	2.021	0.776 ± 0.014
30	96.1	3.495	0.666 ± 0.018
31	150.0	2.363	0.570 ± 0.048
32	199.0	3.291	0.430 ± 0.008
33	23.1	0.888	0.893 ± 0.024
34	39.0	1.480	0.798 ± 0.006
35	247.4	6.381	0.334 ± 0.009

TABLE 3   (continued)

Run	Pressure of Ketene in mm.	Intensity absorbed Einstein x 10^6	$\phi = 1/2 \ \bar{\phi}_{CO}$
48	11.2	0.407	0.841 ± 0.048
49	22.6	0.854	0.798 ± 0.040
50	33.0	1.222	0.763 ± 0.042
51A	43.0	1.516	0.772 ± 0.008
51	52.7	1.879	0.725 ± 0.028
52	99.7	3.203	0.578 ± 0.028
53	151.8	2.807	0.499 ± 0.003
54	199.8	3.788	0.379 ± 0.012

TABLE 4

PHOTOLYSIS OF KETENE AT 3340 $\overset{o}{A}$

Reaction Vessel Temperature   23.0°C

Run	Pressure of Ketene in mm.	Intensity absorbed Einstein x 10^6	$\phi = 1/2 \, \phi_{CO}$
9P	40.1	1.834	$0.556_5 \pm 0.010$
10P	140.1	3.128	$0.327_5 \pm 0.021$
11P	278.8	4.025	0.241 ± 0.005
12P	21.7	1.131	0.626 ± 0.012
13P	186.9	3.998	$0.295_5 \pm 0.006$

TABLE 5

PHOTOLYSIS OF KETENE AT 3340 Å

Reaction Vessel Temperature 0.0°C

Run	Pressure of Ketene in mm.	Intensity absorbed Einstein x 10^6	$\phi = 1/2\,\phi_{CO}$
40	17.2	1.032	0.668 ± 0.003
41	12.8	0.734	$0.699_7 \pm 0.004$
42	24.2	1.462	0.611 ± 0.006
43	34.2	1.551	0.565 ± 0.003
44	44.8	1.613	0.527 ± 0.003
45	87.0	2.087	$0.444_5 \pm 0.017$
47	196.0	3.907	0.249 ± 0.002

TABLE 6

PHOTOLYSIS OF KETENE AT 3650 $\overset{o}{A}$

Reaction Vessel Temperature   23.0°C

Run	Pressure of Ketene in mm.	Intensity absorbed Einstein x 10^6	$\phi = 1/2 \phi_{CO}$ x 10^2
1P	68.4	6.52	0.975 ± 0.099
2P	244.0	14.85	$0.288_5 \pm 0.003$
3P	162.4	10.02	$0.410_5 \pm 0.008$
4P	148.0	7.22	0.460 ± 0.009
5P	28.3	2.91	1.670 ± 0.032
6P	39.4	8.92	1.230 ± 0.072
7P	68.4	4.88	$0.942_5 \pm 0.063$

TABLE 7

RATE CONSTANTS FOR KETENE

λ	$t\,^{\circ}C$	k_{1n}/k_{2n} moles liter^{-1}	k_{1n} (sec^{-1})
3130 $\overset{o}{A}$	23	1.524×10^{-2}	2.523×10^{9}
	0	1.189×10^{-2}	1.885×10^{9}
3340 $\overset{o}{A}$	23	5.373×10^{-3}	8.893×10^{8}
	0	4.175×10^{-3}	6.618×10^{8}
3650 $\overset{o}{A}$	23	4.029×10^{-5}	6.750×10^{6}

TABLE 8

CALCULATED VALUES OF ν, ε_m AND ε_{0-0}

Degrees of Freedom s	ε_m cm^{-1}	ε_{0-0} cm^{-1}	ν sec^{-1}
9	3,980	22,990	6.5×10^{10}
7	4,860	21,260	9.1×10^{10}
5	4,746	21,980	1.4×10^{11}

Predicted values of Porter and Connelly[19]

9	2,360	24,000	1.5×10^{10}

DISCUSSION

1. <u>Theory</u>

The reactions of excited molecules e.g. ketene, can be repre-
sented by the modified Jablonski diagram below.
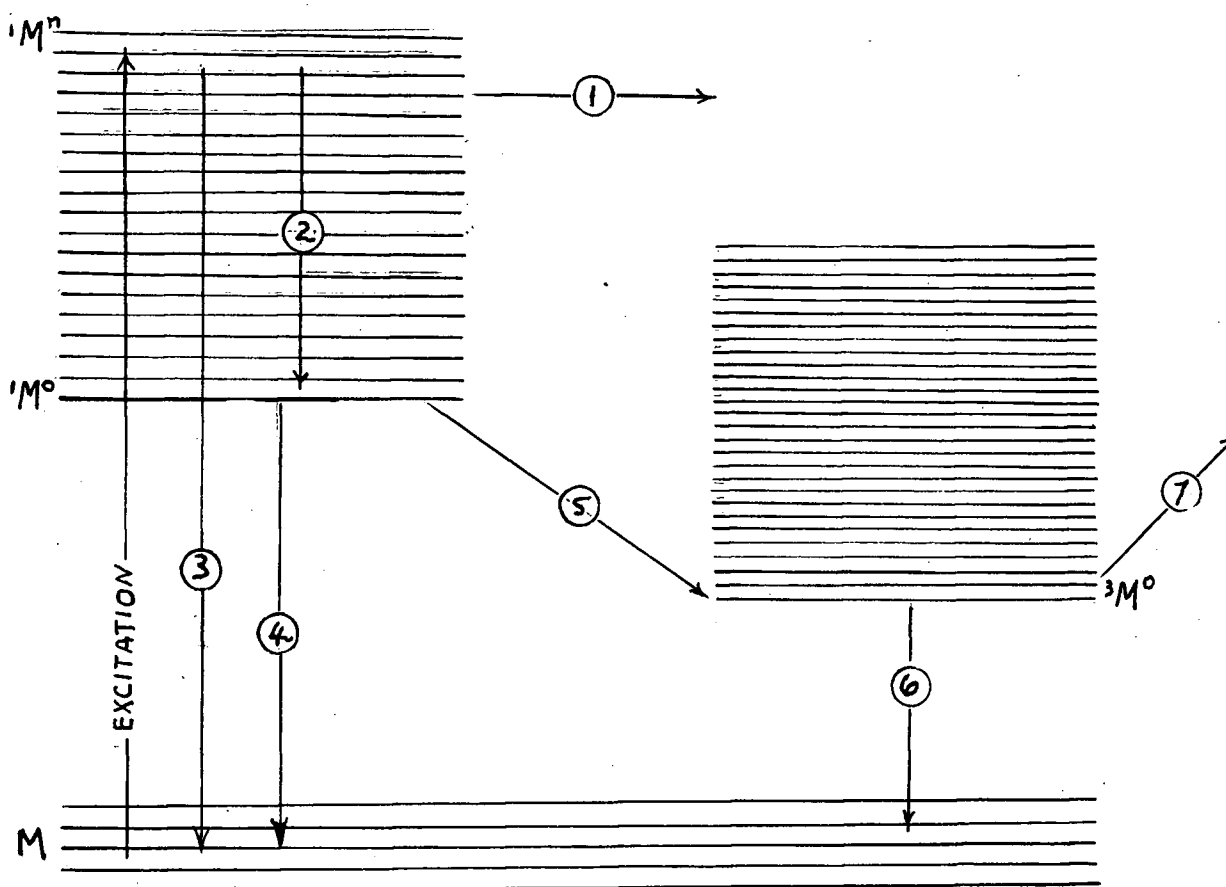
This illustrates the relative energies of the ground electronic state (K),
the first excited singlet state ($^1K^n$) and the first triplet state ($^3K^n$),
n indicating the vibrational energy level.

The reactions can be shown as:

$$K + h\nu \longrightarrow {}^1K^n \qquad\qquad \text{rate} = I_a \qquad (0)$$

$$^1K^n \longrightarrow \text{products} \qquad\qquad \text{rate} = k_{1n}({}^1K^n) \qquad (1)$$

$$^1K^n + K \longrightarrow {}^1K^0 + K \qquad \text{rate} = k_{2n}({}^1K^n)(K) \qquad (2)$$

$$^1K^n \longrightarrow K \qquad\qquad \text{rate} = k_{3n}({}^1K^n) \qquad (3)$$

$$^1K^0 \longrightarrow K \qquad\qquad \text{rate} = k_4({}^1K^0) \qquad (4)$$

$$^1K^0 \longrightarrow {}^3K^0 \qquad\qquad \text{rate} = k_5({}^1K^0) \qquad (5)$$

$$^3K^0 \longrightarrow K \qquad\qquad \text{rate} = k_6({}^3K^0) \qquad (6)$$

$$^3K^0 \longrightarrow \text{products} \qquad\qquad \text{rate} = k_7({}^3K^0) \qquad (7)$$

Reaction (0) depicts absorption and consequent excitation by the incident radiation up to the vibronic state n. In reaction (1) the excited molecule (e.g. ketene) decomposes into products (carbon monoxide and methylene radical). Reaction (2) is a collisional degradation step in which the molecule is degraded in energy to vibronic state 0 and is in vibronic equilibrium, but not electronic, with the surrounding gas.

In some primary quantum yields, extrapolation to zero pressures are less than unity, and hence reaction (3), in which some of the excited molecules in vibronic state n revert to the ground state (an internal conversion process), is included.

Reaction (4), a radiation process e.g. fluorescence, is similar to reaction (3) with reversion from vibronic, but not electronic equilibrium state 0 to the ground state.

Reaction (5) is an inter system crossing from the singlet to the triplet state. It might not be a simple process as shown, but could be a

sequence

$$^1K^0 \longrightarrow \, ^3K^m$$

$$^3K^m + K \longrightarrow \, ^3K^0 + K$$
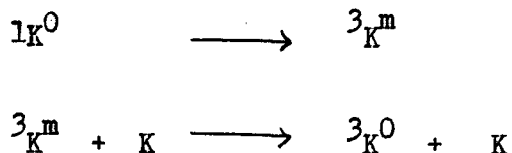
the second reaction being very much faster than the first.

Reaction (6) accounts for phosphorescence, but internal conversion is also included.

Except at very low pressures fluorescence and phosphorescence spectra are known to be independent of the exciting wavelength in the vapor phase, and hence are shown as originating from low vibrational levels of the corresponding excited electronic states.

Increase in primary quantum yields with temperature increase has also been observed and reaction (7), a dissociation from the triplet state, accounts for this.

Dissociation from the $^1K^0$ is excluded as this state (from fluorescence data) has been shown to have a very short lifetime, and so would not exist long enough to be energised by collision and then dissociate. Conversely, however, since phosphorescence is a forbidden transition, the triplet state $^3K^0$ has a long enough lifetime to achieve vibrational equilibrium and dissociate thermally.

If the assumption be made that in a collisional degradation reaction in which all of the effective vibrational energy is removed in one collision i.e. the only vibronic states that dissociate are those reached by an absorption of radiation, a quantum yield relationship may be derived in the following manner.

Rate of product formation $= k_{1n}(^1K^n) + k_7(^3K^0)$ (1)

Rate of formation of

$$\mathbf{1}_K{}^n \quad = \quad I_a - k_{1n}(^1K^n) - k_{2n}(^1K^n)\,(K) - k_{3n}(^1K^n) \qquad (2)$$

Apply steady state conditions, the right hand side of equation (2) is equal to zero. Hence

$$(^1K^n)_{ss} \quad = \quad \frac{I_a}{k_{1n} + k_{2n}(K) + k_{3n}} \qquad (3)$$

Rate of formation of

$$^3K^0 \quad = \quad k_5(^1K^0) - k_6(^3K^0) - k_7(^3K^0) \qquad (4)$$

At steady state conditions

$$(^3K^0)_{ss} \quad = \quad \frac{k_5(^1K^0)}{k_6 + k_7} \qquad (5)$$

Rate of formation of

$$^1K^0 \quad = \quad k_{2n}(^1K^n)\,(K) - k_4(^1K^0) - k_5(^1K^0) \qquad (6)$$

At steady state conditions

$$(^1K^0)_{ss} \quad = \quad \frac{k_{2n}}{k_4 + k_5} \;\; (^1K^n)\,(K) \qquad (7)$$

Substituting equation (7) in (5), we have

$$(^3K^0)_{ss} \quad = \quad \frac{k_5}{k_4 + k_5} \;\cdot\; \frac{k_{2n}}{k_6 + k_7} \;\; (^1K^n)\,(K) \qquad (8)$$

Substitution of equations (3) and (8) in equation (1) gives

Rate of product formation

$$= \frac{k_{1n} I_a}{k_{1n} + k_{2n}(K) + k_{3n}} + \frac{k_7}{k_6 + k_7} \cdot \frac{k_5}{k_4 + k_5} \cdot \frac{k_{2n} I_a(K)}{k_{1n} + k_{2n}(K) + k_{3n}} \quad (9)$$

$$\frac{\text{Rate of product formation}}{I_a} = \phi$$

$$= \frac{k_{1n}}{k_{1n} + k_{2n}(K) + k_{3n}} + \frac{k_7}{k_6 + k_7} \cdot \frac{k_5}{k_4 + k_5} \cdot \frac{k_{2n}(K)}{k_{1n} + k_{2n}(K) + k_{3n}} \quad (10)$$

$$\phi = \left[k_{1n} + ab\, k_{2n}(K)\right] \bigg/ \left[k_{1n} + k_{2n}(K) + k_{3n}\right] \quad (11)$$

where $a = \dfrac{k_5}{k_4 + k_5}$ and $b = \dfrac{k_7}{k_6 + k_7}$

a is then seen to be the fraction of $^1K^0$ molecules which cross to the triplet state and b the fraction of $^3K^0$ molecules which dissociate.

If the simplifying assumption of Ayscough and Steacie[20] be made that k_{3n} is zero, from equation 11 we get

$$\phi = \frac{k_{1n} + ab k_{2n}(K)}{k_{1n} + k_{2n}(K)} \quad (12)$$

$$1 - \phi = \frac{k_{1n} + k_{2n}(K) - k_{1n} - ab k_{2n}(K)}{k_{1n} + k_{2n}(K)}$$

$$= \frac{k_{2n}(K)(1 - ab)}{k_{1n} + k_{2n}(K)} \quad (13)$$

From equations 12 and 13

$$\frac{\phi}{1-\phi} = \frac{k_{1n} + abk_{2n}(K)}{k_{1n} + k_{2n}(K)} \quad x \quad \frac{k_{1n} + k_{2n}(K)}{k_{2n}(K)(1-ab)}$$

$$\frac{\phi}{1-\phi} = \frac{ab}{1-ab} + \frac{k_{1n}}{(1-ab)\,k_{2n}(K)} \tag{14}$$

Hence from equation 14 a plot of $\dfrac{\phi}{1-\phi}$ vs the reciprocal of the

pressure (or concentration) should give a straight line from which ab and

$\dfrac{k_{1n}}{k_{2n}}$ can be evaluated.

Another approximation by Strachan and Noyes[11] neglects reaction

7, triplet dissociation. Hence we have from equation 10

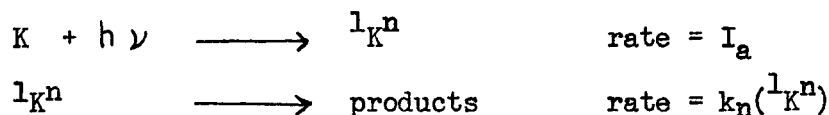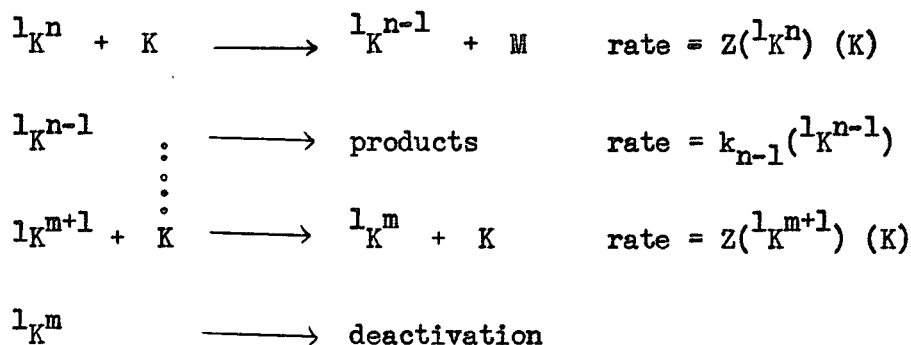$$\phi = \frac{k_{1n}}{k_{1n} + k_{2n}(K) + k_{3n}} \tag{15}$$

and hence

$$\frac{1}{\phi} = 1 + \frac{k_{3n}}{k_{1n}} + \frac{k_{2n}}{k_{1n}}(K) \tag{16}$$

A plot of $\dfrac{1}{\phi}$ vs (K) should then be linear and give values for $\dfrac{k_{3n}}{k_{1n}}$ and

$\dfrac{k_{2n}}{k_{1n}}$.

Deactivation by a Poly-collisional Process.

If the deactivation process involves more than a single collision,

the following mechanism may be postulated

$$K + h\nu \longrightarrow {}^{1}K^{n} \qquad \text{rate} = I_{a}$$

$${}^{1}K^{n} \longrightarrow \text{products} \qquad \text{rate} = k_{n}({}^{1}K^{n})$$

$$^1K^n + K \longrightarrow {}^1K^{n-1} + M \qquad \text{rate} = Z(^1K^n)\,(K)$$

$$^1K^{n-1} \quad \vdots \longrightarrow \text{products} \qquad \text{rate} = k_{n-1}(^1K^{n-1})$$

$$^1K^{m+1} + K \longrightarrow {}^1K^m + K \qquad \text{rate} = Z(^1K^{m+1})\,(K)$$

$$^1K^m \longrightarrow \text{deactivation}$$

The indexes m and n are measures of the vibrational energy of the excited singlet state, m + 1 being the lowest state from which dissociation will take place.

For simplicity if reaction 3 is omitted and steady state treatment be applied, the concentrations of the various states are

$$k_j(^1K^j)_{ss} = I_a \frac{a_j}{(K)} \prod_{i=j}^{i=n} \frac{1}{1 + \frac{a_i}{(K)}} \tag{17}$$

where $a_i = \dfrac{k_i}{Z}$

and then

$$\phi_j = \frac{k_j(^1K^j)}{I_a} = \frac{a_j}{(K)} \prod_{i=j}^{i=n} \frac{1}{1 + \frac{a_i}{(K)}} \tag{18}$$

The sum of contributions from each vibronic state would then be the primary quantum yield of dissociation (with dissociation from only the singlet state).

$$\phi = \sum_{j=m+1}^{j=n} \frac{a_j}{(K)} \prod_i^n \frac{1}{1 + \frac{a_i}{(K)}} \tag{19}$$

Since the total quantum yield cannot exceed unity, equation (19) can then be written

$$\phi = 1 - \prod_{m+1}^{n} \frac{1}{1 + \frac{a_i}{(K)}} \tag{20}$$

where $\prod_{m+1}^{n} \frac{1}{1 + \frac{a_i}{(K)}}$ is the quantum yield from the

m + 1 vibronic state.

If thermal dissociation from the triplet state is now included, the total quantum yield for dissociation is now given by

$$\phi = 1 - (1 - ab) \prod_{m+1}^{n} \frac{1}{1 + \frac{a_i}{(K)}} \tag{21}$$

where a and b are the quantities defined in equation (11).

In order to evaluate equations (20) and (21) the unimolecular theory of dissociation[21-23] is assumed to apply to photochemical processes, since experimental data have indicated that the rate of dissociation of excited vibronic states is a function of their energy content. The rate constant for dissociation from each vibronic state is then expressed as

$$k_i = \nu (1 - \frac{\mathcal{E}_m}{\mathcal{E}_i})^{s-1} \tag{22}$$

where ν, evaluated from its value $\frac{kT}{h}$ in Eyring's theory, or the weighted root-mean-square of the normal mode frequencies of vibration in Slater's theory, has the approximate value of 10^{13} sec^{-1}. $\mathcal{E}_i$ and $\mathcal{E}_m$ are the vibrational energies corresponding to states of index m and i respectively.

s is the nondegenerate modes of vibration in the molecule and k_i is the

specific rate constant of vibrational state i of energy $\mathcal{E}_i$. From this

the quantity a_i can be calculated.

In order to simplify the calculations, it is assumed that each

collision results in the loss of a constant amount of vibrational energy,

hence, that the vibrational energy is proportional to the indexes n, m etc.

In ketene the maximum degrees of freedom is 9 and hence s = 9. Assuming

$\mathcal{V} = 10^{13}$ sec^{-1} and $Z = 10^{11}$ mole^{-1} liter sec^{-1}, $\dfrac{\mathcal{V}}{Z}$ is equal to 100 mole

liter^{-1}. Values of $\dfrac{k_i}{Z}$ can then be calculated.

When values of ϕ are calculated from equation (20), it is found

that with excitation energies only slightly greater than the minimum energy

required for dissociation, the reciprocal of the primary quantum yield is

linear with pressure. For higher energies e.g. n $\rangle$ 44 and m = 30 the

curves were linear only at very high pressures. At low pressures they were

concave upwards and had a zero slope at zero pressure.

If the relative number of collisions is varied i.e. if calcu-

lations are made with different values of m, the results are as shown in

Figure 4. It can be seen that an increase in the number of collisions requir-

ed for degradation, i.e. a decrease in the vibrational energy removed in each

collision, greatly increases the primary quantum yield. There is a marked

departure from linearity of the reciprocal quantum yield vs. pressure, and

also a higher extrapolated quantum yield at zero pressure.

Variation of the degrees of freedom s causes the primary quantum

yield to change as illustrated in Figure 5, the slope increasing with an

increase of s.

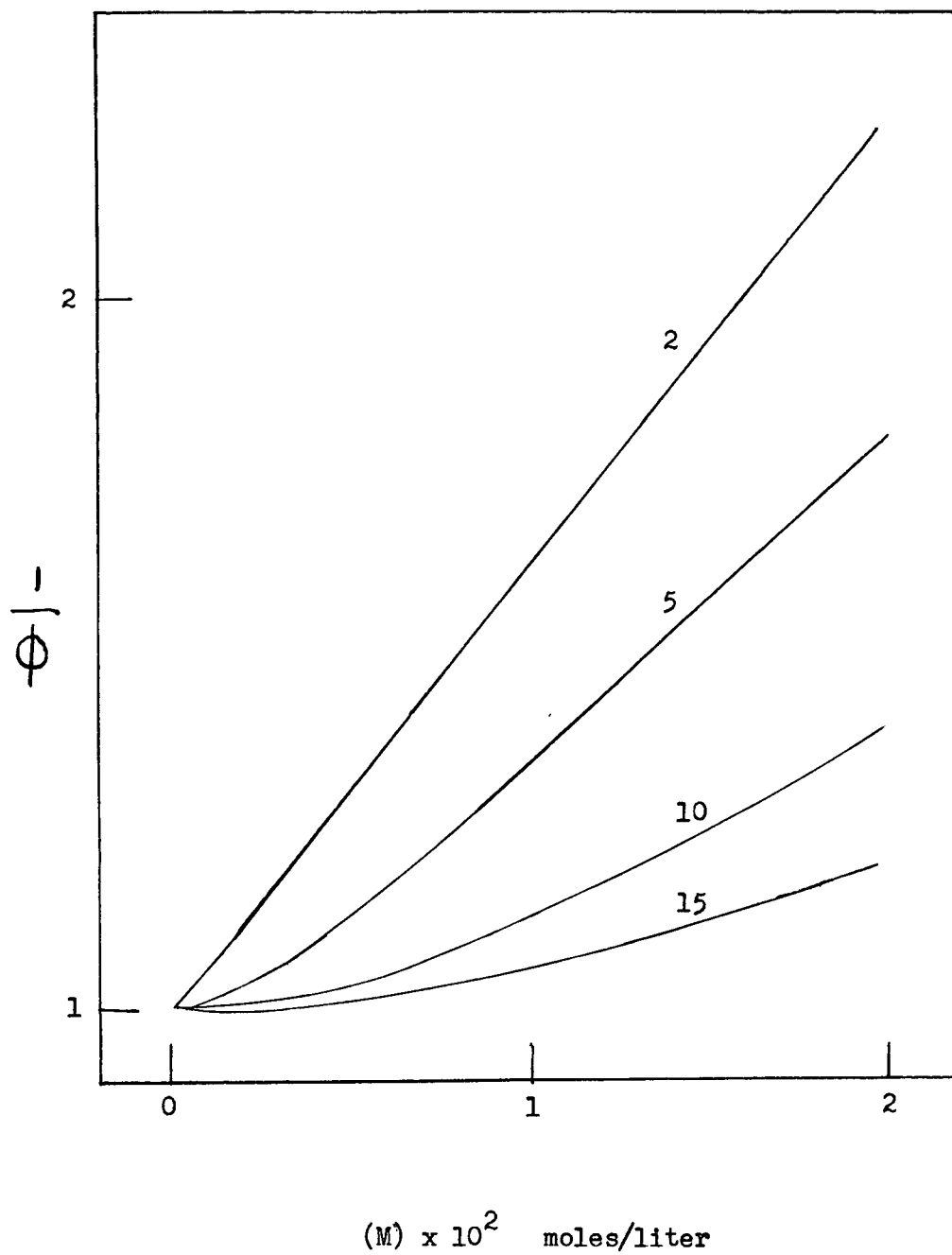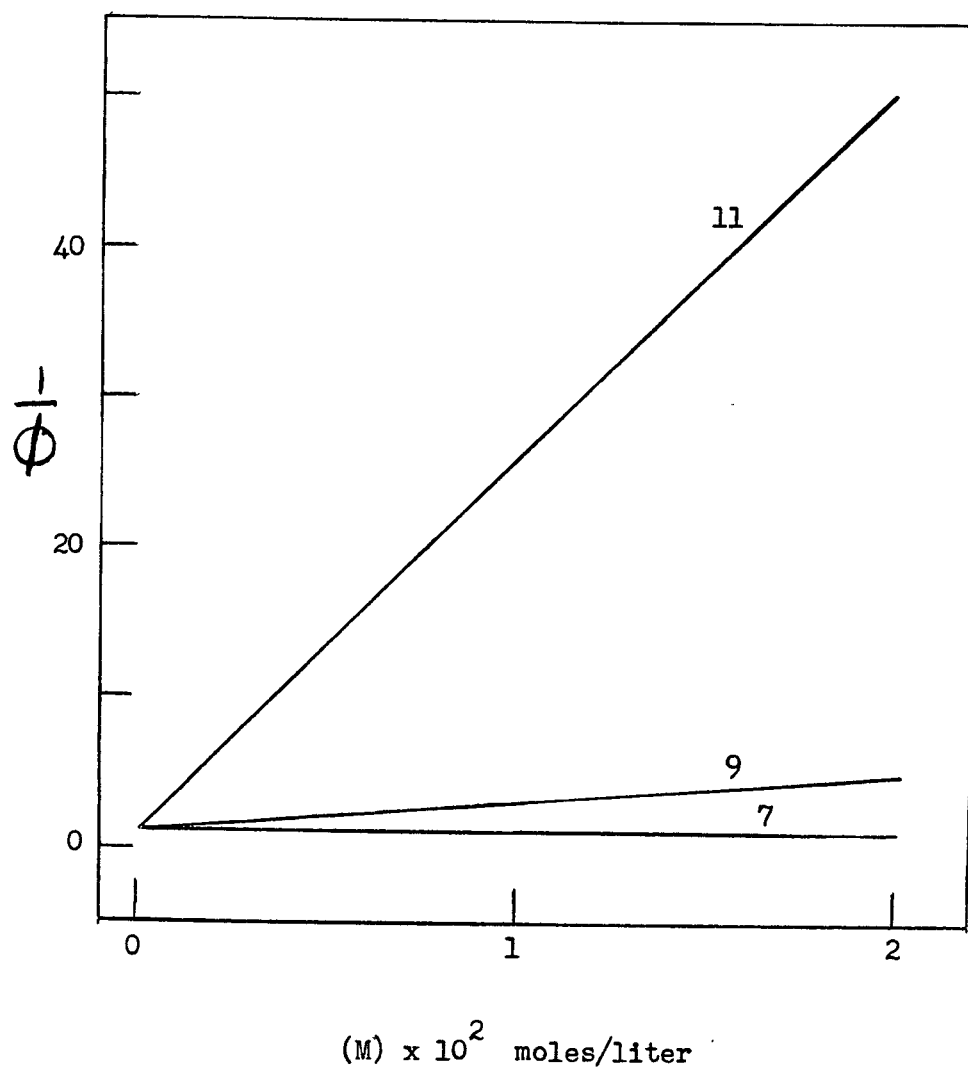FIGURE 4. Calculated quantum yield, s = 9, n/m = 1.5, m = 2, 5, 10, and 15.

FIGURE 5. Calculated quantum yield, n = 41, m = 30,
s = 7, 9, and 11.

(M) x 10^2 moles/liter

If calculations are made using equation (21), i.e. if thermal dissociation from the triplet state is included, the results are as illustrated in Figure 6. A radical change is observed in the curves. They are concave downward, becoming "S" shaped with larger values of ab, an effect which appears even at low pressures.

2. Experimental Data

The calculations from the above theories can now be compared with the experimental data.

At a wavelength of 3130 $\overset{o}{A}$ and T = 23°C, the variation of quantum yield with pressure is shown in Figure 7. The curve is seen to be linear over the range of pressures used and extrapolation to zero pressure yields an intercept of 1.00 within the experimental error. This data can then be assumed to fit the equation

$$1/\phi = 1 + \frac{k_{2n}}{k_{1n}} (K) \tag{23}$$

and the kinetics then be represented by equations (0), (1), (2). It is likely then within experimental error, that at 3130 $\overset{o}{A}$ internal conversion and collisional deactivation of the excited molecule are, if any, very small contributing factors.

For 3340 $\overset{o}{A}$ and 3650 $\overset{o}{A}$ at 23°C results from the data in Tables 4 and 6 are shown in Figures 8 and 9. From Figure 8 it is seen that at 3340 $\overset{o}{A}$ the intercept is 1.45 and the slope is greater than at 3130 $\overset{o}{A}$. At 3650 $\overset{o}{A}$ the intercept is 19.70 and the slope is about thirteen times as much as at 3340 $\overset{o}{A}$.

FIGURE 6. Calculated quantum yield, including thermal
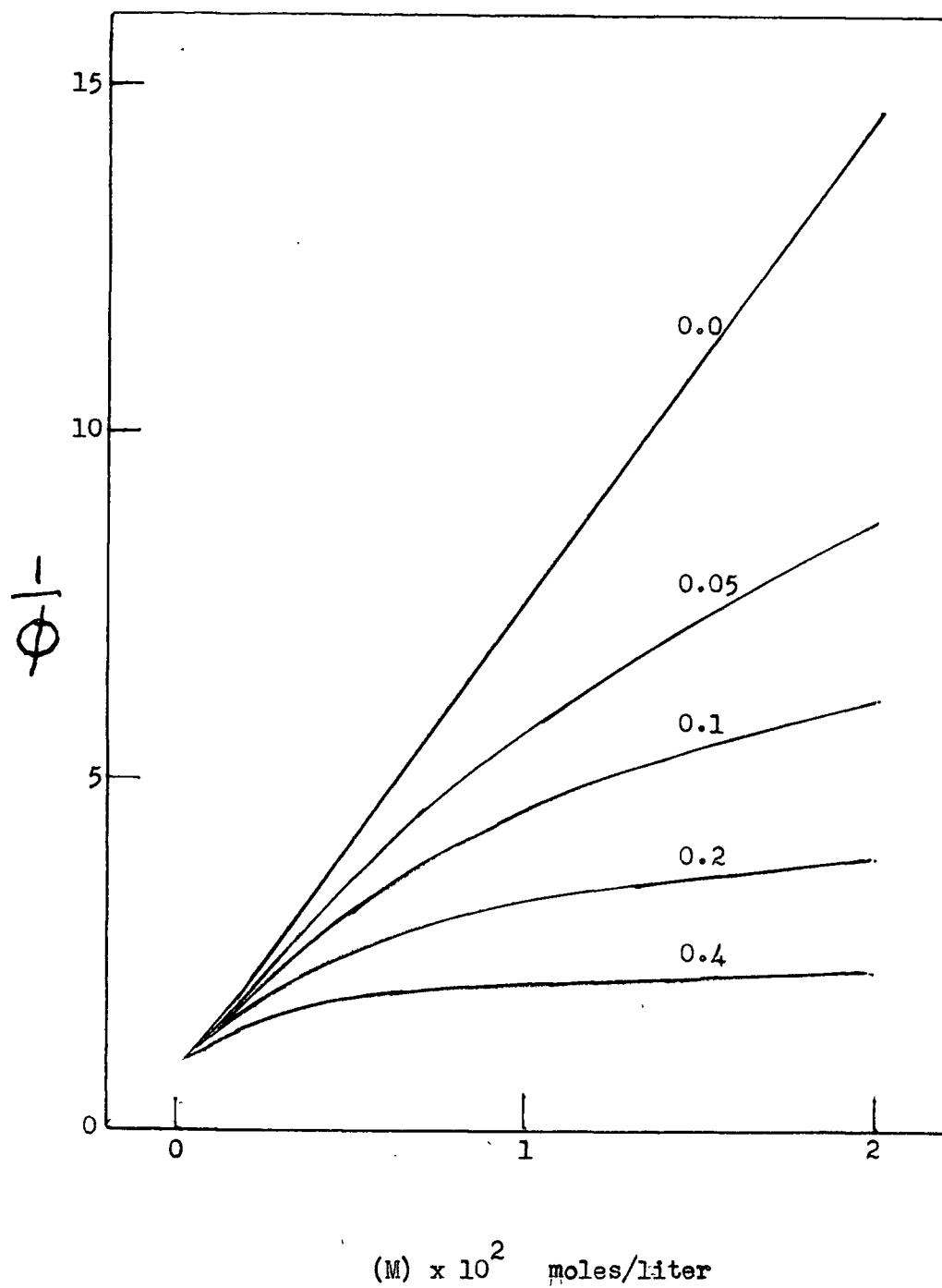dissociation of triplet molecules, n = 39, m = 30, s = 9
ab = 0, 0.05, 0.1, 0.2, 0.4.

FIGURE 7. Dependence of Primary Quantum Yield on Pressure at 3130 $\overset{o}{A}$ and 23°C.
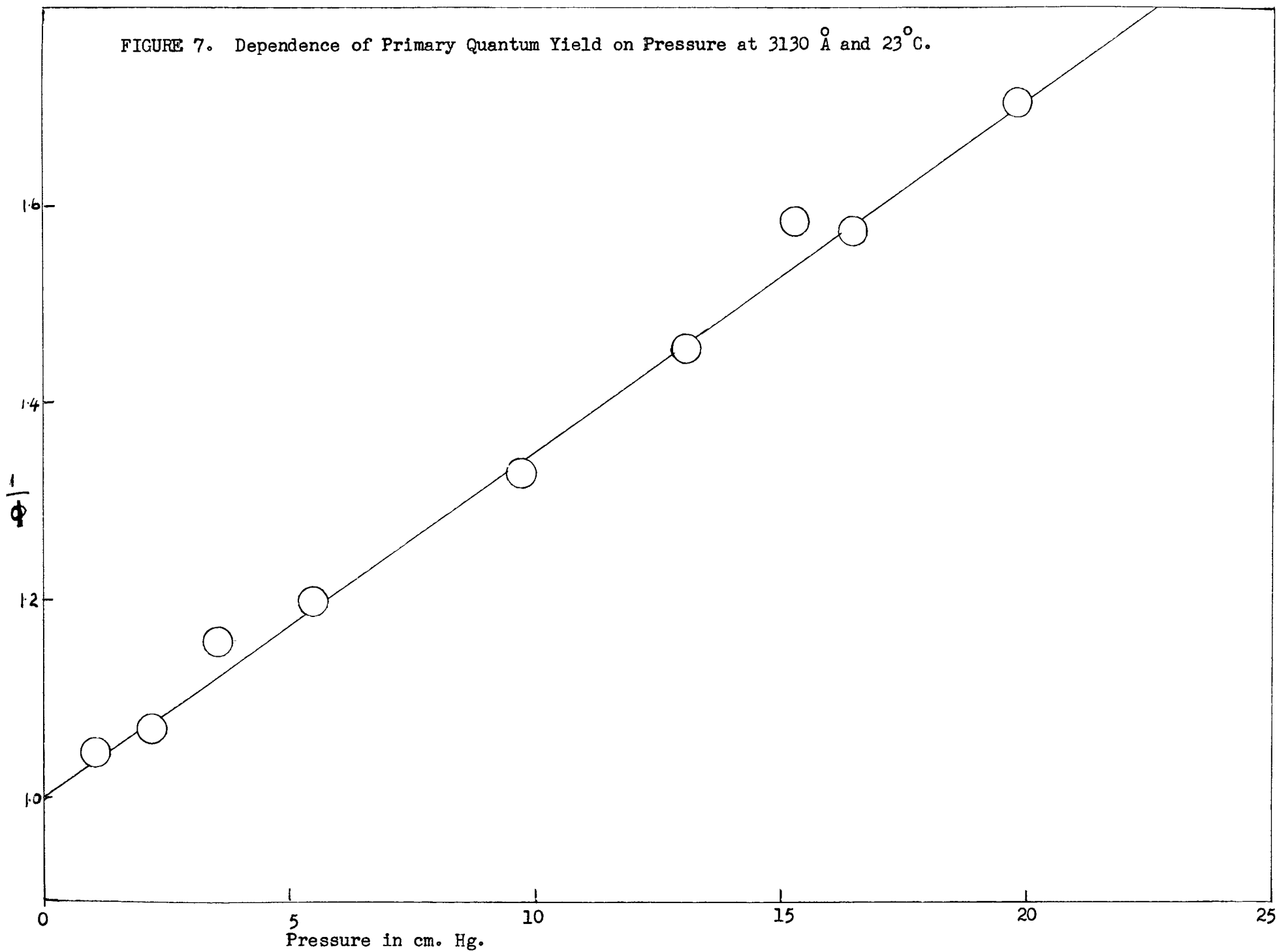
39b

FIGURE 8. Dependence of Primary Quantum Yield on Pressure at 3340 Å and 23°C.
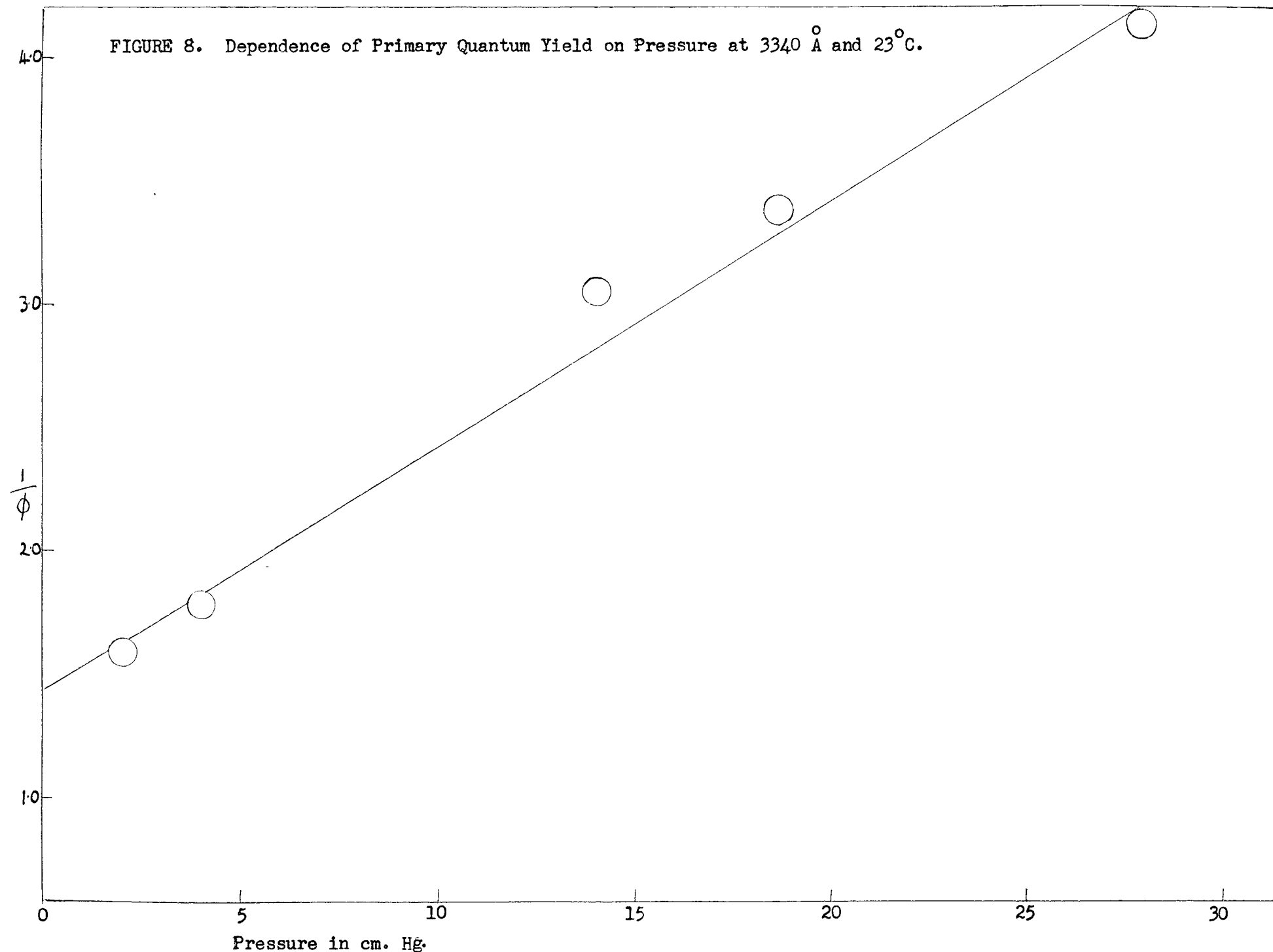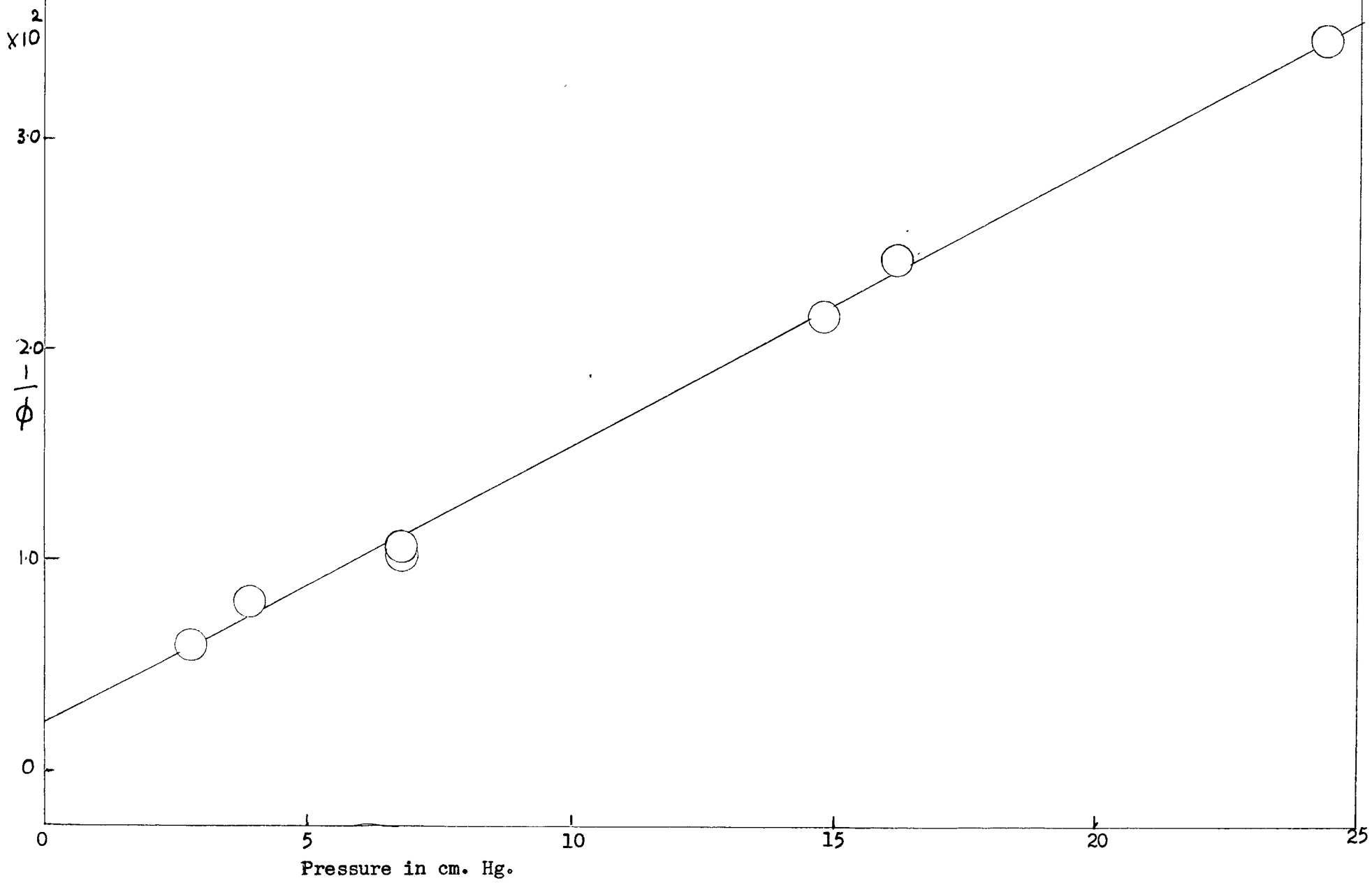
Pressure in cm. Hg.

FIGURE 9.   Dependence of Primary Quantum Yield on Pressure at 3650 Å and 23°C.

The data at 3340 Å and 3650 Å can then be assumed to be represented by the equation

$$1/\phi = 1 + \frac{k_{3n}}{k_{1n}} + \frac{k_{2n}}{k_{1n}} \quad (K)$$

which is equation (16) and hence the kinetics could be approximately represented by reactions (0), (1), (2), (3).

The increase of intercepts and slopes of the curves with increase of wavelength indicates that at longer wavelengths, internal conversion and collisional deactivation of the excited molecules are of increasing importance. Apparently at the longer wavelengths the lifetime of the excited state is longer than at shorter wavelengths, so that deactivation rather than dissociation can take place.

From the quantum yields at the various wavelengths, it can be seen that there is a marked decrease with increasing wavelength. Examination of Figures 7, 8, and 9 which give plots of the inverse quantum yields vs. pressure at $23^{\circ}C$ and Figures 10 and 11 which are for $0^{\circ}C$, also shows a decided variation in the slopes of the curves.

For 3130 Å at $23^{\circ}C$ the slope is 0.656×10^2 liter moles^{-1}. At $0^{\circ}C$ it has increased to 0.841×10^2 liter moles^{-1}.

For 3340 Å at $23^{\circ}C$ the slope is 1.861×10^2 liter moles^{-1} and 2.395×10^2 at $0^{\circ}C$.

For 3650 Å at $23^{\circ}C$ it is 2.482×10^4 liter moles^{-1}.

From this it can be seen that the effect of temperature variation follows the opposite pattern of the effect of varying the wavelength. Thus low temperature effects can be compared with the effects of longer wavelengths, while high temperature effects on the quantum yields are similar to the effects of shorter wavelengths. The quantum yields are lowered as

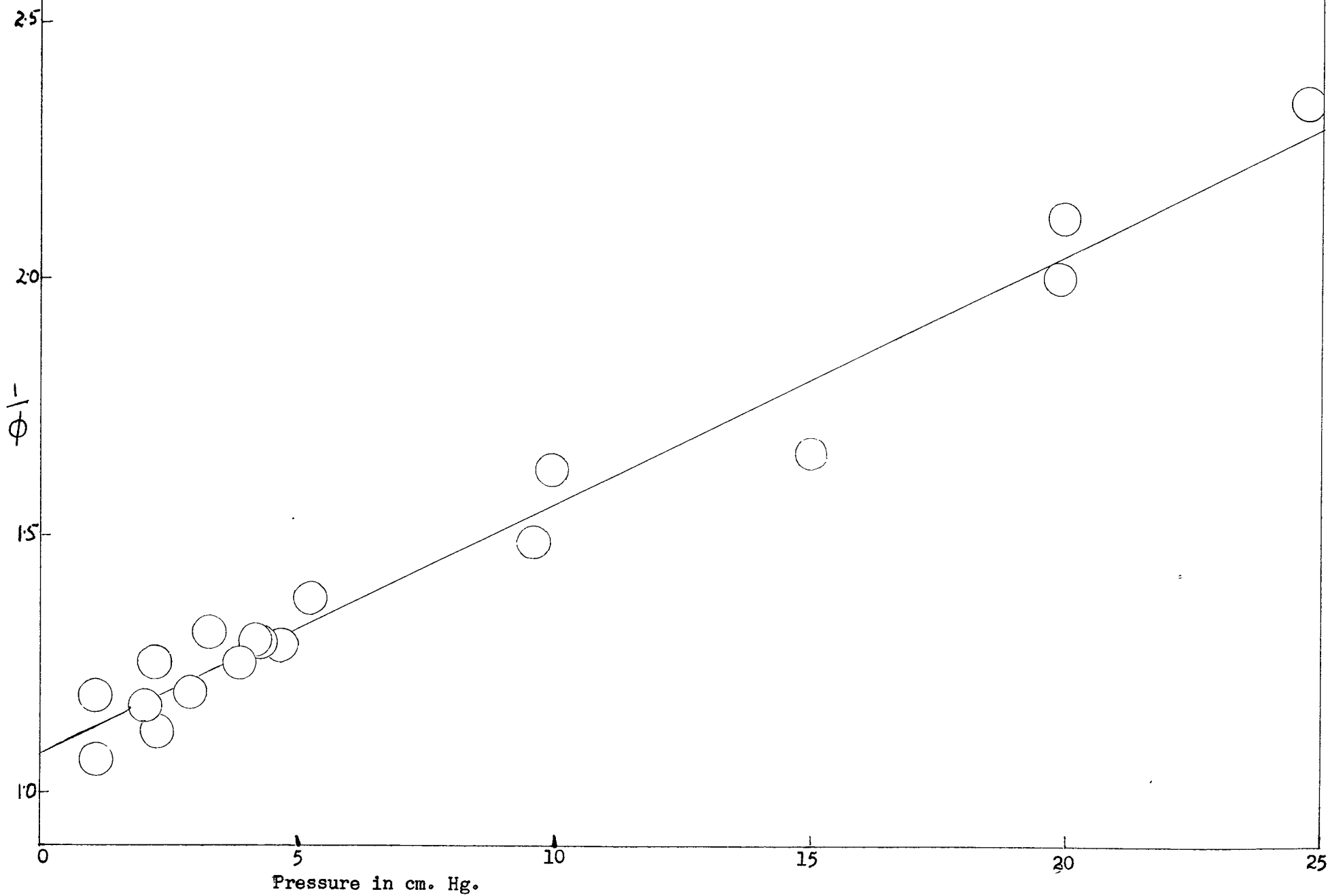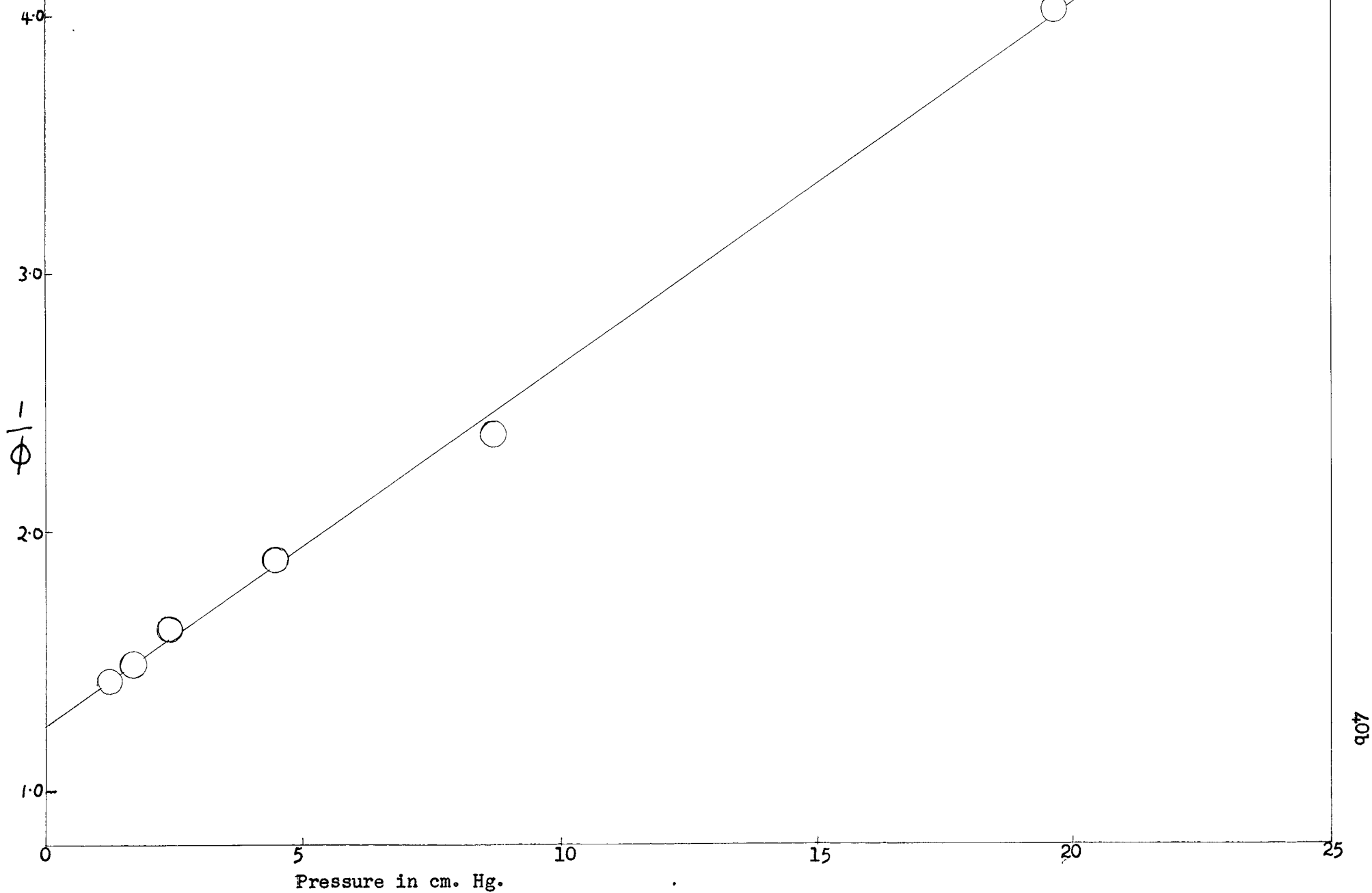FIGURE 10. Dependence of Primary Quantum Yield on Pressure at 3130 Å and 0°C.

FIGURE 11. Dependence of Primary Quantum Yield on Pressure at 3340 Å and 0°C.

the wavelength is increased or as the temperature is decreased, and are greater with shorter wavelengths or higher temperature.

This relationship can be interpreted by reference to Figure 12 where the various energies are qualitatively related.

Curves I and II represent the distribution of the energies of the molecules at temperatures T_1 and T_2, T_2 being greater than T_1. Curves I^* and II^* represent the distribution of energy after absorption of the exciting radiation by the molecules.

From curves I and II it can be seen that the average energy of the molecules E_2 avg. at temperature T_2 is greater than the average energy E_1 avg. at temperature T_1.

Examination of the excited curves I^* and II^* shows the average energy E_2 avg. at T_2 greater than E_1 avg. at T_1. This means that $\mathcal{E}_2$ (see Figure 12), which represents the average energy of the excited state above the $\mathcal{E}_{0-0}$ energy at T_2 is greater than $\mathcal{E}_1$, the average energy above $\mathcal{E}_{0-0}$ energy at T_1.

Both $\mathcal{E}_1$ and $\mathcal{E}_2$ correspond to $\mathcal{E}_i$ in the Kassel unimolecular theory of dissociation as given by equation (22). The greater the value of $\mathcal{E}_i$ the greater will be k_i, the rate of dissociation. Consequently, because of the difference in $\mathcal{E}_1$ and $\mathcal{E}_2$ ($\mathcal{E}_2 \rangle \mathcal{E}_1$) the quantum yield from the higher temperature T_2 will be greater (indicated by a smaller slope of $1/\phi$ vs. pressure), than at T_1.

If the temperatures T_1 and T_2 are decreased, both the excited curves I and II will be compressed towards the left, thus decreasing $\mathcal{E}_1$ and $\mathcal{E}_2$, and a smaller quantum yield is to be expected since k_i from

$$k_i = \nu(1 - \frac{\mathcal{E}_m}{\mathcal{E}_i})^{s-1}$$

FIGURE 12. Diagram of Molecular Energies at T_1 and T_2 (T_2 T_1)
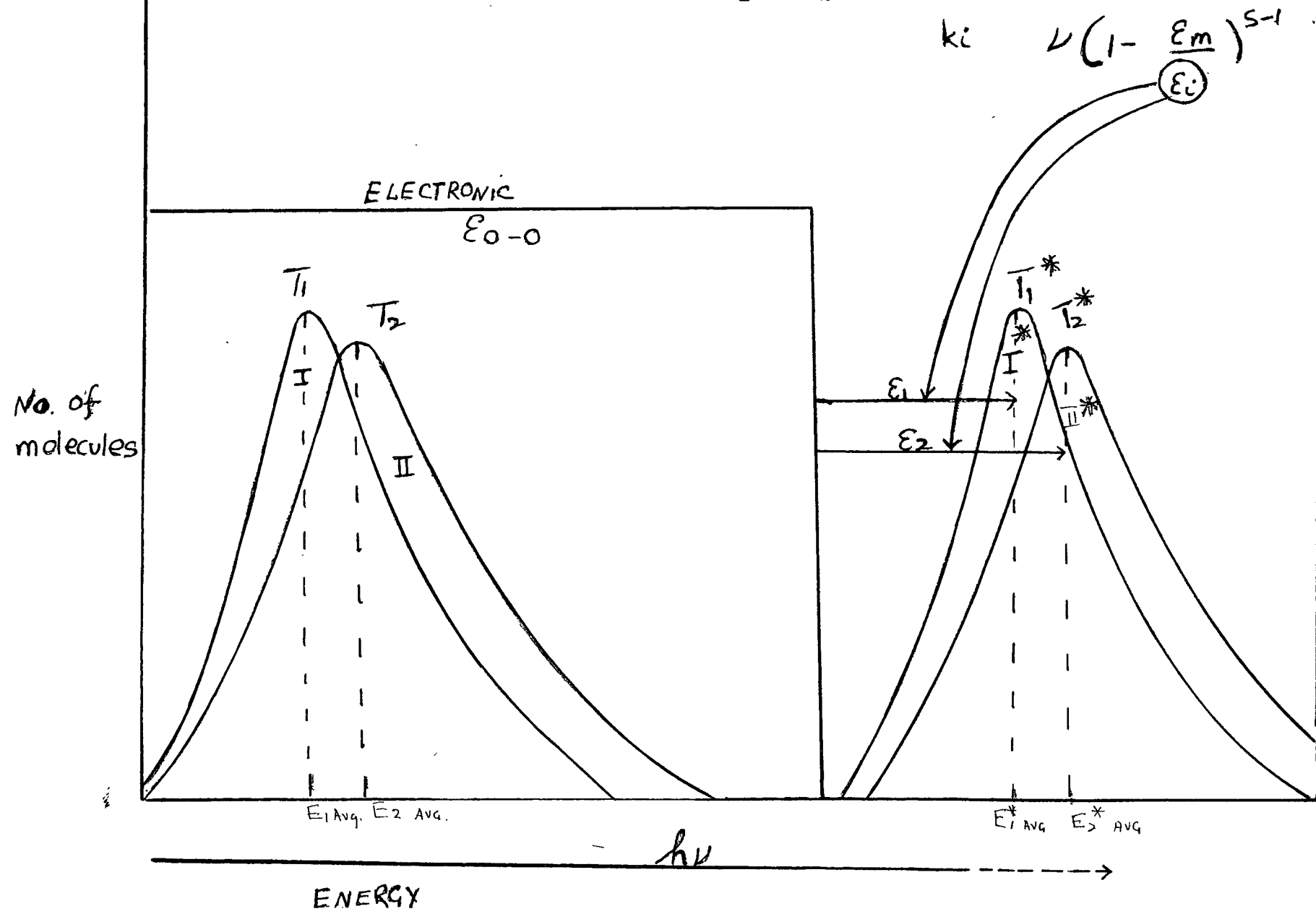
will be smaller, i.e. less dissociation occurs.

The effect of wavelength is similarly related. Since the ε_{0-0} energy is independent of wavelength the values of ε_1 and ε_2 depend on $h\nu$, the energy of the exciting radiation. Consequently, with longer wavelengths, i.e. excitation with lower energy radiation, the values of ε_1 and ε_2 will be smaller (the excited curves I^* and II^* will shift towards the left), than with shorter or more energetic wavelengths (the excited curves I^* and II^*, then shifting towards the right, thus increasing ε_1 and ε_2). Hence, there will be a decrease in the rate of dissociation k_i from the above relationship, and smaller quantum yields at longer wavelengths are to be expected. Examination of all the plots of $1/\phi$ vs. pressure, shows the curves to be all linear within the limit of experimental error. Consequently, the kinetics of equation (21) do not seem to be applicable. The curves do not show the "S" shape as predicted from triplet dissociation contribution to the quantum yields. Hence it can be concluded that dissociation from the triplet state does not play a significant part in the photo-dissociation process.

From Figure 4 which is predicted by equation (20) involving a cascade collisional degradation process, it can be seen that for m = 2 or less the curves of $1/\phi$ vs. pressure are linear while at m = 5 or more, there is a decided departure from linearity. The concavity effect between m = 2 to 4, is small. Consequently within the experimental limits, it is not possible to distinguish between the kinetics of a 1, 2 or 3 collisional degradation process. However, it can be qualitatively stated that there are not more than about 3 collisions involved in the deactivation process.

In Table 7 are the inverse slopes (= $\frac{k_{1n}}{k_{2n}}$) obtained from the curves $1/\phi$ vs. pressure at the different wavelengths and temperatures.

If 4 $\overset{\text{o}}{\text{A}}$ is chosen as the collision diameter of ketene and k_{2n} = Z the values

of k_{1n} in column 4 of Table 7 are found. The value of Z obtained from

$$Z = \sigma^2 \left(\frac{8 \pi kT}{\mu} \right)^{1/2}$$

where σ = collision diameter

μ = reduced mass of ketene = $\frac{MW}{2}$

was 1.655 x 10^{11} liter mole^{-1} sec^{-1} at 23$^{\text{o}}$C and was 1.585 x 10^{11} liter mole^{-1}
sec^{-1} at 0$^{\text{o}}$C.

These values can now be applied to the unimolecular theory of

dissociation given by equation (22). Calculations of the quantities ν, $\mathcal{E}_m$

and $\mathcal{E}_{0-0}$ give the values shown in Table 8 for various degrees of freedom

s (maximum value = 9).

These show very good agreement with the theoretical values of

Porter and Connelly[19]. The total energy, electronic and vibrational ($\mathcal{E}_{0-0}$

+ $\mathcal{E}_m$), which is virtually independent of parameters in the theory is

25970 cm^{-1} (s = 9), 26120 cm^{-1} (s = 7) and 26726 cm^{-1} (s = 5), which corre-

spond to 74.2 k cals/mole, 74.6 k cals/mole and 76.3 k cals/mole respect-

ively, in good agreement with the value of 76.3 k cals/mole obtained by

Porter and Connelly[19]. As the carbon-carbon bond energy in ketene is about

55 k cals/ mole, the photodissociation must lead to excited products.

Since the vibrational frequencies of ketene are known, it is

possible to calculate the heat capacity, $C_{vib.}$ The value is 210 cm^{-1} for

27$^{\text{o}}$ to 154$^{\text{o}}$C or 4.72 cals. deg.$^{-1}$ mole^{-1}. From the photochemical data the

effective heat capacity, $C_{eff.}$ can also be calculated. The values obtained

are 74.3 cals. deg.$^{-1}$ mole^{-1} with 3130 $\overset{\text{o}}{\text{A}}$ and 42.9 cals. deg.$^{-1}$ mole^{-1} with

3340 $\overset{\text{o}}{\text{A}}$. It is seen that the $C_{eff.}$ is very much greater than $C_{vib.}$ obtained

from thermochemical calculations.

This result is not unexpected. The thermochemical calculations concern average energies of molecules, but the photochemical data are based on energies weighted with respect to dissociation. Hence for the latter, the molecules having high energies are more important than those with average energies. This is analogous to a thermal dissociation in which the rate constant is an exponential function of temperature, while the average energy is approximately a linear function of temperature.

BIBLIOGRAPHY

1. Norrish, R.G.W., Crone, H.G. and Saltmarsh, O.D., J. Chem. Soc. 1533 (1933).

2. Ross, W.F. and Kistiakowsky, G.B., J. Am. Chem. Soc. 56, 1112 (1934).

3. Pearson, T.G., Purcell, H. and Saigh, G.S., J. Chem. Soc. 409 (1938).

4. Rosenblum, C., J. Am. Chem. Soc. 63, 3322 (1941).

5. Burton, M., Davis, T.W., Gordon, A. and Taylor, H.A., J. Am. Chem. Soc. 63, 1956 (1941).

6. Rice, F.O. and Glasebrook, A.L., J. Am. Chem. Soc. 56, 2381 (1934).

7. Kistiakowsky, G.B. and Rosenberg, N.W., J. Am. Chem. Soc. 72, 321 (1950).

8. Vanpee, M. and Grard, F., Ann. Min. Belg. 49, 701 (1950).

9. Vanpee, M. and Grard, F., Bull. Soc. Chim. Belg. 60, 208 (1951).

10. Kistiakowsky, G.B. and Marshall, W.L., J. Am. Chem. Soc. 74, 88 (1952).

11. Strachan, A.N. and Noyes, W.A., J. Am. Chem. Soc. 76, 3258 (1954).

12. Noyes, W.A., Porter, G.B. and Jolley, E.J., Chem. Revs. 56, 49 (1956).

13. Porter, G.B., J. Am. Chem. Soc. 79, 827 (1957).

14. Connelly, B.T. and Porter, G.B., Can. J. Chem. 36, 1640 (1958).

15. Kistiakowsky, G.B. and Mahan, B.H., J. Am. Chem. Soc. 79, 2412 (1957).

16. Fisher, G.J., MacLean, A.F. and Snizer, A.W., J. Org. Chem. 18, 1055, (1953).

17. Davis, W., J. Am. Chem. Soc. 70, 1868 (1948).

18. Hatchard, C.G. and Parker, C.A., Proc. Roy. Soc. (London) A235, 518 (1956).

19. Porter, G.B. and Connelly, B.T., J. Chem. Phys. 33, 81 (1960).

20. Ayscough, P.B. and Steacie, E.W.R., Proc. Roy. Soc. (London) A234, 476 (1956).

21. Kassel, L.J., Kinetics of Homogeneous Gas Reactions. (Chemical Catalog Company, New York, 1932).

BIBLIOGRAPHY (continued)

22. Glasstone, S., Laidler, K.J. and Eyring, H., _The Theory of Rate Processes_. (McGraw-Hill Book Company, Inc., New York, 1941).

23. Slater, N.B., Proc. Roy. Soc. (London) _A194_, 112 (1948).